



PROGETTO AdSP n. 1951

Estensione delle infrastrutture comuni per lo sviluppo del Punto Franco Nuovo nel porto di Trieste

CUP: C94E21000/ 60001

Progetto di Fattibilità Tecnico Economica Fascicolo A- intervento PNC da autorizzare

GRUPPO DI PROGETTAZIONE:		
arch. Gerardo Nappa	AdSP MAO	Responsabile dell'integrazione e Coordinatore per la Sicurezza in fase di Progettazione
arch. Sofia Dal Piva	AdSP MAO	Progettazione generale
arch. Stefano Semenic	AdSP MAO	Progettazione generale
ing. Roberto Leoni	BITECNO S.r.l.	Sistema di trazione elettrica ferroviaria
ing. Saturno Minnucci	MINNUCCI ASSOCIATI S.r.l.	Impianti speciali e segnalamenti ferroviari
ing. Dario Fedrigo	ALPE ENGINEERING S.r.l.	Progettazione strutturale oo.cc. ferrovia e strade
ing. Andrea Guidolin p.i. Furio Benci	SQS S.r.l.	Progettazione della sicurezza
ing. Sara Agnoletto	HMR Ambiente S.r.l.	Progettazione MISP e cassa di colmata
p.i. Trivellato, dott. G. Malvasi, dott. S. Bartolomei	p.i. Antonio Trivellato d.i.	Modellazione rumore, atmosfera, vibrazioni
dott. Gabriele Cailotto ing. Anca Tamasan	NEXTECO S.r.l.	Studio di impatto ambientale e piano di monitoraggio ambientale
ing. Sebastiano Cristoforetti	CRISCON S.r.l.s.	Relazione di sostenibilità
ing. Tommaso Tassi	F&M Ingegneria S.p.A.	Progettazione degli edifici pubblici nel contesto dell'ex area "a caldo"
ing. Michele Titton	ITS s.r.l.	Connessione stradale alla GVT
RESPONSABILE UNICO DEL PROCEDIMENTO: ing. Paolo Crescenzi		

NOME FILE: <i>IGNR_P_R_M-MAR_3AM_001_04_00.docx</i>	SCALA: ---
TITOLO ELABORATO: STUDIO METEOMARINO parte 2 di 3	ELABORATO: <i>IGNR_P_R_M-MAR_3AM_001_04_00</i>

Rev.	Data	Descrizione	Redatto	Verificato	Approvato
00	01/02/2023	Definitivo	DHI	S.Dal Piva	G.Nappa

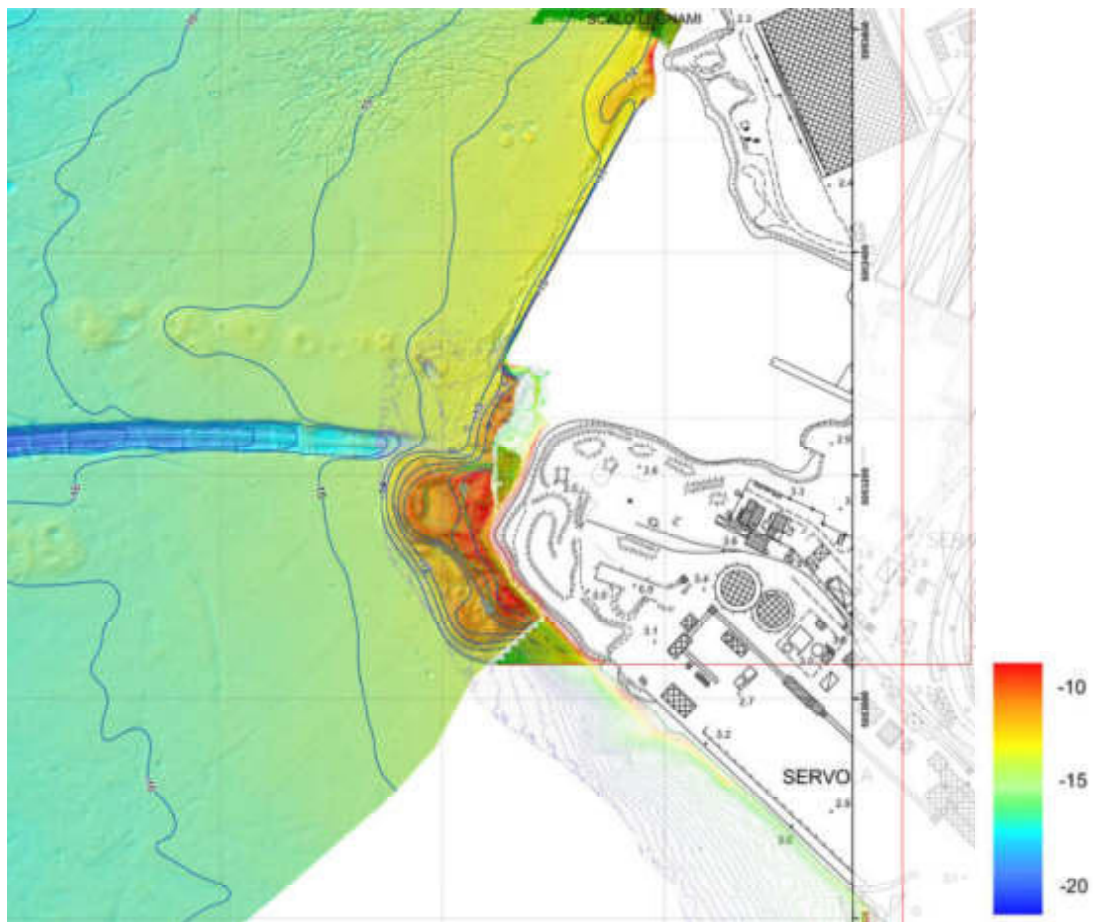


Figura 9-4 *Mappa batimetrica del bacino di evoluzione del Molo VII redatta da OGS per l'AdSP Mar Adriatico Orientale nel 2019*

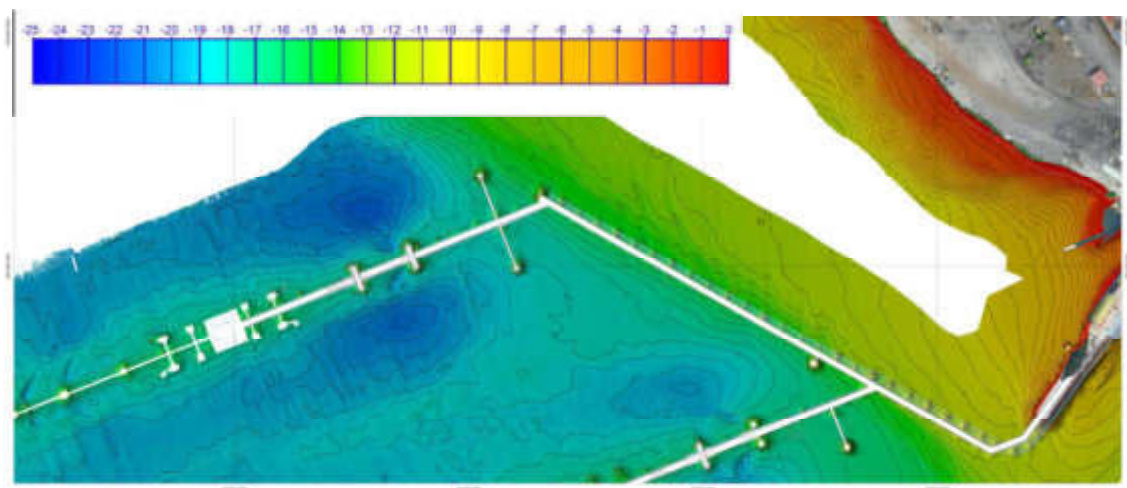


Figura 9-5 *Planimetria stato dei luoghi con isobate passo 0.5 m redatta da Subsea Fenix per conto di Prisma Srl, all'interno del "Rilievo e monitoraggio dello stato di conservazione delle banchine dell'area marina e costiera di competenza dell'Autorità di Sistema Portuale del Mare Adriatico Orientale" nel Marzo 2021*

	Progetto integrato di messa in sicurezza, riconversione industriale e sviluppo economico produttivo nell'area della ferriera di Servola Relazione Tecnica	Pag. 149 di 157
--	--	--------------------

Infine, si evidenzia che è ancora oggi visibile la depressione creatasi intorno al relitto della nave Wien che, nel 1917, durante la I Guerra Mondiale, venne affondata a meno di mezzo miglio di distanza dalla Ferriera di Servola, ad una profondità di circa 20 m. Nel 1925 vennero recuperati alcuni pezzi della nave, ma la demolizione del relitto proseguì fino agli anni '50, quando fu utilizzato anche l'esplosivo per il recupero. Questa circostanza è un'ulteriore dimostrazione di come il trasporto e l'accumulo di sedimenti nel tempo in questa area risulti assai modesto.

9.4 Considerazioni finali sulla sedimentazione nel bacino portuale

L'analisi sopra descritta permette di concludere che i fenomeni di risospensione dei sedimenti e di successivo deposito degli stessi all'interno dell'area portuale, ed in particolare nell'intorno della porzione di fondale per la quale è previsto l'escavo nell'ambito del progetto siano da considerarsi trascurabili.

Una movimentazione locale e difficilmente predicibile potrebbe tuttavia essere indotta dalle eliche delle navi in evoluzione / accosto o che attraversano il bacino portuale. Si suggerisce pertanto un periodico monitoraggio delle quote del fondale finalizzato alla manutenzione ottimale dei fondali nelle aree interessate dai lavori di escavo.

	Progetto integrato di messa in sicurezza, riconversione industriale e sviluppo economico produttivo nell'area della ferriera di Servola Relazione Tecnica	Pag. 150 di 157
--	--	--------------------

10 CONCLUSIONI

All'interno del Porto di Trieste è prevista, in corrispondenza della Piattaforma Logistica PLT, un'espansione verso mare delle infrastrutture a servizio del porto mediante la realizzazione di un molo fondato su pali, ai quali sarà affidata la funzione di sostenere l'impalcato del nuovo Terminal, comprensivo del nuovo fronte banchinato a Nord-Ovest, lungo il quale è previsto l'ormeggio di navi di più grandi dimensioni, tali da richiedere l'escavo dei fondali.

Un team di progettazione multidisciplinare ha sviluppato il progetto integrato relativo alla nuova opera marittima e alle annesse infrastrutture stradali e ferroviarie, secondo una pianificazione che si sviluppa su più fasi successive. Nell'ambito di questo ampio progetto è inserito lo Studio di Impatto Ambientale che deve comprendere, tra i vari studi specialistici, l'analisi degli effetti, sia in fase di cantiere che di esercizio, della realizzazione della nuova opera sull'idrodinamica e la qualità delle acque nella baia di Muggia; le attività sono state sviluppate mediante l'applicazione di opportuna modellistica numerica.

La prima fase è stata dedicata alla raccolta ed analisi dei dati disponibili per la caratterizzazione del sito: dati batimetrici e granulometrici, dati di circolazione generale del Golfo di Trieste, condizioni di marea, condizioni atmosferiche e di moto ondoso, nonché individuazione dei corsi d'acqua che sfociano nel bacino portuale e degli habitat marini sensibili presenti.

Successivamente, è stato implementato il modello idrodinamico MIKE 3 HD - *Hydrodynamics*, annidato al modello di larga scala *Mediterranean Sea Physics Reanalysis* disponibile nell'ambito del Servizio Europeo CMEMS. L'applicazione di questo modello tridimensionale ad alta risoluzione ha permesso di ricavare i campi di corrente, temperatura, salinità e livelli su una finestra temporale di un anno (Settembre 2014 - Settembre 2015). Il periodo di simulazione è stato selezionato in funzione della disponibilità di campagne di misura di temperatura e salinità lungo la colonna d'acqua, disponibili per alcuni punti all'interno del bacino di Muggia e messi a disposizione da parte di OGS - Istituto Nazionale di Oceanografia e di Geofisica Sperimentale (campagne di Settembre 2014, Gennaio e Marzo 2015); tali dati sono stati anche utilizzati per la validazione del modello. Il modello ha mostrato un'idrodinamica molto variabile lungo la colonna d'acqua: in superficie le correnti prevalenti (più intense e frequenti) sono dirette verso Sud-Ovest, mentre al fondo hanno una direzione prevalente opposta. In superficie le velocità sono mediamente più elevate, dell'ordine di circa 5 cm/s, rispetto al fondo, dove le correnti hanno intensità medie di 2 cm/s.

Si evidenzia che per la ricostruzione della circolazione all'interno del porto di Trieste si è ritenuto trascurabile il contributo dato dalle onde sull'idrodinamica costiera. Questa assunzione è stata opportunamente verificata mediante un preliminare studio di propagazione delle onde da largo verso l'interno della baia e da una successiva analisi delle condizioni idrodinamiche generate da eventi rappresentativi per il sito in studio.

Il modello idrodinamico è stato successivamente dinamicamente accoppiato a due distinte tipologie di modello: MIKE 3 AD - *Advection-Dispersion*, il modello che permette di calcolare l'evoluzione di un ipotetico tracciante per avvezione-dispersione, ed il modello MIKE 3 MT - *Mud Transport*, per lo studio del trasporto, dispersione e sedimentazione dei sedimenti fini.

	Progetto integrato di messa in sicurezza, riconversione industriale e sviluppo economico produttivo nell'area della ferriera di Servola Relazione Tecnica	Pag. 151 di 157
--	--	--------------------

Questi modelli sono stati applicati seguendo un approccio a "finestre mobili", in piena conformità alle indicazioni riportate nelle linee guida ISPRA di settore. Questa metodologia consiste nell'implementare un alto numero di simulazioni di trasporto, che coprono un periodo di tempo inferiore all'anno e che vengono replicate più volte, in maniera tra loro indipendente, in modo da coprire l'intero periodo preso a riferimento per le condizioni idrodinamiche di circolazione.

Il modello MIKE 3 AD è stato applicato per la valutazione dell'impatto della presenza della nuova infrastruttura sull'idrodinamica della baia (fase di esercizio). L'approccio seguito è stato quello di imporre in uno specifico volume di controllo una concentrazione di un ipotetico tracciante pari a 100 e di simularne i tempi di abbattimento, sia nella configurazione attuale (assenza dei pali di fondazione della nuova infrastruttura) che in quella di progetto (presenza dei suddetti pali). Come volumi di controllo sono stati considerati sia l'intera baia di Muggia, sia il solo bacino dell'Arsenale S. Marco e dello Scalo Legnami, posto a Nord del futuro Molo VIII, la cui idrodinamica sarà maggiormente interessata dalla presenza della nuova infrastruttura. Questa applicazione ha consentito di ottenere le "curve di ricambio idrico", ossia curve che indicano la percentuale di volume d'acqua che viene ricambiato nel tempo. Il confronto di queste curve, ottenute in presenza ed in assenza dei pali, hanno permesso di valutare l'entità dell'impatto dell'opera sulla circolazione ed il ricambio idrico. Per questo studio si è fatto riferimento a due periodi idrodinamici reali medio-lunghi pari a 30 giorni, uno rappresentativo del periodo invernale (elevato idrodinamismo e colonna d'acqua completamente rimescolata) ed uno rappresentativo del periodo estivo (scarso idrodinamismo e significativa stratificazione termica della colonna d'acqua). I periodi sono stati selezionati sulla base di un'analisi anemometrica, mantenendo come anno di riferimento quello simulato in precedenza con il modello idrodinamico (Settembre 2014 - Settembre 2015). Il modello di avvezione-dispersione è stato dinamicamente accoppiato al modello idrodinamico secondo un approccio a "finestre mobili", ossia simulazioni della durata di 15 giorni, ma sfasate tra loro di 24 ore, al fine di coprire l'intero mese preso a riferimento.

I risultati hanno mostrato che le differenze tra lo stato attuale e quello di progetto sono assai modeste: esse risultano del tutto trascurabili se si fa riferimento al ricambio idrico dell'intera baia per il mese estivo preso a riferimento. Le differenze risultano lievemente superiori, ma comunque molto piccole, sempre inferiori al 3%, se si fa riferimento al bacino dell'Arsenale S. Marco e dello Scalo Legnami (estate e inverno) o al ricambio idrico dell'intera baia per il mese invernale considerato. E' possibile pertanto affermare che la presenza dei pali di fondazione dell'impalcato della nuova infrastruttura (stralcio del Molo VIII previsto dal Piano Regolatore Portuale) comporta un impatto trascurabile sulla circolazione generale e, di conseguenza, sui tempi di ricambio dei bacini interessati.

Per lo studio dell'impatto della nuova infrastruttura in fase di cantiere è stato applicato il modello MIKE 3 MT, che ha permesso di quantificare l'incremento di torbidità delle acque marine dovuto alle operazioni che prevedono la movimentazione dei sedimenti. Queste operazioni possono essere distinte in due diverse fasi: quella di realizzazione dei pali, per la quale sono stati simulati sia gli effetti dell'escavo all'interno delle "camicie" che ospiteranno i getti di calcestruzzo, sia gli effetti del getto stesso, e quella di dragaggio della porzione di fondale, in corrispondenza del nuovo fronte banchinato a Nord Ovest, dove ormeggeranno le navi di più grandi dimensioni.

In virtù della prevista durata complessiva delle lavorazioni (circa 3 anni per la realizzazione dei pali e circa 5 mesi per il dragaggio), il modello è stato implementato per un periodo più breve,

	Progetto integrato di messa in sicurezza, riconversione industriale e sviluppo economico produttivo nell'area della ferriera di Servola Relazione Tecnica	Pag. 152 di 157
--	--	--------------------

rappresentativo (secondo un approccio conservativo) di una fase delle lavorazioni durante la quale la movimentazione dei sedimenti avverrà nella zona più prossima ai target ambientali (habitat marini) e laddove l'idrodinamismo (e quindi la possibilità di maggiore dispersione del sedimento movimentato) è maggiore. In particolare, sulla base delle informazioni operative fornite, sono state assunte alcune ipotesi di lavoro che hanno portato alla determinazione del tasso di produttività (o *rate* di dragaggio) per entrambe le fasi di lavoro, nonché all'individuazione della finestra temporale di riferimento più opportuna in funzione delle lavorazioni previste (individuata in 28 giorni per la fase di realizzazione dei pali e a 30 giorni per la fase di dragaggio).

Le simulazioni di trasporto di sedimento sono state dinamicamente accoppiate alla simulazione idrodinamica realistica di lungo periodo (un anno) secondo l'approccio a "finestre mobili", ossia si è ipotizzato che le operazioni abbiano inizio il giorno 1 ed il giorno 15 di ogni mese, in modalità separata, cosicché una simulazione non interferisca con la precedente e con la successiva. I risultati, distinti per le diverse operazioni, sono stati ottenuti in termini di mappe delle massime concentrazioni di sedimento sospeso in colonna d'acqua, di tempi di superamento di una determinata soglia di concentrazione e di accumulo di sedimento al fondo.

Per quanto riguarda la fase di realizzazione dei pali, dal momento che l'escavo ed il successivo getto di calcestruzzo avvengono all'interno delle "camicie" preventivamente infisse, si è ipotizzato che la fuoriuscita di sedimento avvenga solo in corrispondenza dello strato superficiale. I risultati mettono pertanto in evidenza che in superficie il pennacchio di torbida è in generale più esteso rispetto agli strati più profondi della colonna d'acqua: mentre in superficie le concentrazioni superano i 2 mg/l (concentrazione diffusamente considerata corrispondente ad acqua limpida) all'interno del bacino portuale, senza comunque oltrepassare le dighe foranee, e rimanendo piuttosto confinate nella zona centrale della baia, senza interessare la fascia costiera a Sud, al fondo le concentrazioni sono superiori ai 2 mg/l solo nell'intorno dello scavo, fino ad una distanza massima di circa 1 km. Come atteso, le concentrazioni di sedimento più elevate si hanno nell'intorno del punto di rilascio dei sedimenti; allontanandosi, il pennacchio di sedimenti assume una forma allungata in direzione Nord-Ovest Sud-Est, seguendo l'andamento delle correnti. Dal punto di vista della persistenza, in superficie la concentrazione di 2 mg/l viene superata per più di 3 ore (sui 28 giorni simulati) nella zona centrale del bacino portuale, mentre al fondo, a parte la zona interessata dalle operazioni, la persistenza è in generale inferiore alle 3 ore. L'area interessata da questo deposito dei sedimenti rilasciati dalle operazioni di realizzazione dei pali è piuttosto modesta: un accumulo di sedimenti superiore a 0.5 mm si verifica in una zona con estensione pari a circa 1000 m in direzione parallela a costa e pari a circa 500 m nella direzione trasversale.

L'escavo del fondale in corrispondenza del nuovo fronte banchinato a Nord-Ovest verrà eseguito con draghe meccaniche con benne a tenuta, per cui la perdita di sedimento (ridotta rispetto alle benne tradizionali ma qui comunque considerata cautelativamente pari al 3% del volume dragato) avviene in maniera uniformemente distribuita lungo la colonna d'acqua. Questo fa sì che il pennacchio di sedimenti sospesi abbia, alle diverse profondità, una variabilità ridotta. Si osserva però che l'estensione del pennacchio e le concentrazioni sono più elevate al fondo rispetto alla superficie; questo perché, negli strati più profondi, al materiale perso dalla benna in risalita lungo la colonna d'acqua a quella specifica profondità, si aggiunge il materiale perso negli strati sovrastanti, che progressivamente precipita verso il fondo. In superficie, le concentrazioni superano i 2 mg/l solo all'interno del bacino portuale: il pennacchio delle concentrazioni massime

	Progetto integrato di messa in sicurezza, riconversione industriale e sviluppo economico produttivo nell'area della ferriera di Servola Relazione Tecnica	Pag. 153 di 157
--	--	--------------------

lambisce le dighe foranee ad Ovest e la costa nelle altre direzioni. Al fondo questo pennacchio si sviluppa maggiormente verso il largo; infatti, si riscontrano concentrazioni superiori ai 2 mg/l anche poco oltre le dighe foranee. Come atteso, le concentrazioni massime più elevate si hanno nell'intorno della zona dragata; allontanandosi dall'area delle lavorazioni il pennacchio di sedimenti assume una forma allungata in direzione Nord-Ovest Sud-Est, seguendo l'andamento delle correnti. Dal punto di vista della persistenza, per la maggior parte del bacino la concentrazione di 2 mg/l viene superata per più di 24 ore (sui 30 giorni simulati), ma al di fuori delle dighe foranee la persistenza è al di sotto delle 3 ore. L'area interessata dal deposito dei sedimenti è anche in questo caso piuttosto modesta: un accumulo di sedimenti superiore a 0.5 mm si verifica in una zona con estensione pari a circa 1400 m in direzione parallela a costa e pari a circa 700 m nella direzione trasversale.

I risultati del modello hanno permesso inoltre di affermare che le condizioni potenzialmente più svantaggiose per gli habitat marini si verificano quando, dopo un lungo periodo a basso idrodinamismo, durante il quale i sedimenti che vengono messi in sospensione durante le lavorazioni permangono più a lungo in colonna d'acqua, si presenta una condizione che determina un'accelerazione della corrente (tipicamente l'innesco di condizioni di vento intenso da Bora). Questa condizione fa sì che si crei una circolazione tale da trasportare verso la zona dove sono localizzati gli habitat non solo i sedimenti messi in sospensione in quelle ore di lavorazione, ma anche una parte di volume di sedimento non ancora completamente precipitato e ancora presente in colonna d'acqua. Questa situazione, che è pertanto la più svantaggiosa, porta comunque a valori massimi di sedimento sospeso in corrispondenza degli habitat (in particolare nella zona ove dovrebbe essere presente la *pinna nobilis*) molto bassi, pari a circa 3 mg/l e per un periodo di tempo di poche ore. Si evidenzia che questa condizione si verifica solo durante la fase di escavo dei fondali, in quanto durante la fase di realizzazione dei pali non si evidenzia in alcun modo un effetto "cumulo" tra due cicli di lavoro successivi, debolmente presente, invece, per la fase di escavo dei fondali.

I risultati mostrano pertanto che gli effetti derivanti dalla movimentazione di sedimenti in fase di cantiere sono sostanzialmente trascurabili in corrispondenza degli habitat marini sensibili presenti nella baia di Muggia e, più in generale, nella porzione di Golfo di Trieste più prossima al porto. Il pennacchio di torbida non arriva a toccare le zone ad Ovest di Porto San Rocco, sia perché questa fascia risulta protetta dalla presenza delle strutture del porto, sia perché, trovandosi in prossimità della bocca Sud del bacino, essa è soggetta a correnti più intense che pertanto disperdono più velocemente il sedimento.

I risultati della modellazione non suggeriscono pertanto la necessità di impiego di particolari misure di mitigazione, quali le panne anti-torbidity, volte a contenere i sedimenti rilasciati in colonna d'acqua durante le lavorazioni. Ove tale soluzione fosse comunque indicata dagli Enti ad ulteriore cautela, anche in considerazione della classificazione del porto di Trieste come Sito di Interesse Nazionale (SIN), si ritiene utile già in questa sede suggerire l'impiego di panne anti-torbidity limitate agli strati più superficiali, in virtù sia delle ridotte concentrazioni di sedimento attese, sia del basso livello di idrodinamismo che caratterizza la baia di Muggia con particolare riferimento agli strati intermedi e profondi della colonna d'acqua.

	Progetto integrato di messa in sicurezza, riconversione industriale e sviluppo economico produttivo nell'area della ferriera di Servola Relazione Tecnica	Pag. 154 di 157
--	--	--------------------

11 RIFERIMENTI

- [1] I., Lisi; A., Feola; A., Bruschi; M., Di Risio; A., Pedroncini; D., Pasquali; E., Romano, *La modellistica matematica nella valutazione degli aspetti fisici legati alla movimentazione dei sedimenti in aree marino-costiere. Manuali e Linee Guida ISPRA, 169/2017, pp.144., 2017.*
- [2] Autorità Portuale di Trieste, Technital, AcquaTecno, «Piano Regolatore Portuale del Porto di Trieste,» in *Studio Ambientale Integrato - Quadro di Riferimento Progettuale, 2013.*
- [3] Istituto Nazionale di Oceanografia e di Geofisica Sperimentale (OGS) - Sezione di ricerca tecnologica IRI - Gruppo LIAD, «Porto di Trieste - Elaborazione di dati batimetrici,» Borgo Grotta Gigante, 16 dicembre 2019.
- [4] Subsea Fenix S.r.l., «Planimetria stato dei luoghi con isobate passo 0.25 m,» *Rilievo e monitoraggio dello stato di conservazione delle banchine dell'area marina e costiera di competenza dell'Autorità di Sistema Portuale del Mare Adriatico Orientale, Marzo-Maggio 2021.*
- [5] Jeppesen Marine, «CM-93, Global Electronic Chart Database Professional+,» Jeppesen Marine, Norway, 2016.
- [6] DHI, «MIKE C-MAP, Extraction of World Wide Bathymetry Data and Tidal Information, Scietific Documentation,» MIKE by DHI, Hørsholm, 2021.
- [7] L.G.T. Laboratorio Geotecnico S.r.l., Prove su terre - Area Marino Costiera antistante l'ex area a caldo della Ferriera di Servola, Trieste, 2021.
- [8] Copernicus, «Marine Copernicus Services,» Copernicus, 2021. [Online]. Available: <https://www.copernicus.eu/en/copernicus-services/marine>.
- [9] CMEMS Copernicus Marine Service Information, «Mediterranean Sea Physics Reanalysis,» [Online]. Available: https://doi.org/10.25423/CMCC/MEDSEA_MULTIIYEAR_PHY_006_004_E3R1.
- [10] G. Madec, «NEMO (Nucleus for European Modelling of the Ocean) ocean engine,» *Note du Pôle de modélisation, Institut Pierre-Simon Laplace (IPSL), vol. 27 ISSN, pp. 1288-1619, 2008.*
- [11] CMEMS - Copernicus Marine Environment Monitoring Service, «Quality Identification Document (QUID) - Global Ocean Physics Reanalysis,» Global High Resolution Production Centre, 29 04 2021. [Online]. Available:

	Progetto integrato di messa in sicurezza, riconversione industriale e sviluppo economico produttivo nell'area della ferriera di Servola Relazione Tecnica	Pag. 155 di 157
--	--	--------------------

<https://catalogue.marine.copernicus.eu/documents/QUID/CMEMS-GLO-QUID-001-030.pdf>.

- [12] M. Tsimplis, R. Proctor e R. Flather, «A two-dimensional tidal model for the Mediterranean Sea,» *Journal of Geophysical Research*, vol. 100, Agosto 1995.
- [13] C. Yongcun e O. Baltazar Andersen, «Improvement in global ocean tide model in shallow water regions,» in *Poster, SV.1-68 45, OSTST*, Lisbon, Oct.18-22, 2010.
- [14] ARPA FVG, OSMER e GRN, «Osservatorio meteorologico regionale del FVG,» [Online]. Available: <https://www.osmer.fvg.it/archivio.php?ln=&p=dati>. [Consultato il giorno 2021].
- [15] Saha, Suranjana e Coauthors, «The NCEP Climate Forecast System Reanalysis,» *Bull. Amer. Meteor. Soc.*, pp. 91, 1015.1057. doi: 10.1175/2010BAMS3001.1, 2010.
- [16] NCEP - National Centre for Environmental Prediction, «The GFS Atmospheric Model,» 28 August 2003. [Online]. Available: <http://www.emc.ncep.noaa.gov/gmb/moorthi/gam.html>.
- [17] Riserva Naturale Val Rosandra, Parchi e Riserve Naturali FVG, Comune di San Dorligo della Valle, Piano di conservazione e sviluppo della riserva naturale regionale della Val Rosandra, Dolina, 2020.
- [18] Geokarst Engineering Srl; GSSG - Gruppo Speleologico San Giusto, «Test di tracciamento nella "Fessura del Vento" in Val Rosandra (Carso triestino),» in *Incontro Internazionale di Speleologia "Esplorando"*, S. Omobono Imagna Terme, 28-31 ottobre 2005.
- [19] ARPA FVG, Provincia di Trieste, Applicazione dell'Indice di Funzionalità Fluviale (IFF) al Rio Osopo e confronto dei risultati ottenuti con quelli del 2002, 2016.
- [20] C. D'Ambrosi e F. Mosetti, Contributi alle conoscenze geo-idrologiche della Piana di Zaule., 1962.
- [21] A. Pedroncini, G. Contento, L. Donatini, L. Cusati, G. Lupieri, H. Hansen e R. Bolanos Sanches, «Mediterranean Wind Wave Model (MWM): a 42 year hindcast database of wind and wave conditions and a base for relocatable operational forecast models,» 2021.
- [22] DHI, «MIKE 21 SW - Spectral Wave Module, Scientific Documentation,» MIKE by DHI, Hørsholm, 2021.
- [23] DHI, «MIKE 3 Flow Model HD FM, Hydrodynamics Flexible Mesh, Scientific Documentation,» MIKE by DHI, Hørsholm, 2021.

	Progetto integrato di messa in sicurezza, riconversione industriale e sviluppo economico produttivo nell'area della ferriera di Servola Relazione Tecnica	Pag. 156 di 157
--	--	--------------------

- [24] DHI, «MIKE 21/3 Flow Model HD FM, Hydrodynamics Flexible Mesh, Scientific Documentation,» MIKE by DHI, Hørsholm, 2021.
- [25] R. Flather, «A tidal model of the northwest European continental shelf,» *Memories de la Societe Royale des Sciences de Liege*, vol. 6, n. 10, p. 141-164, 1976.
- [26] DHI, «MIKE 21 AD FM - Advection Dispersion Flexible Mesh, Scientific Documentation,» MIKE by DHI, Hørsholm, 2020.
- [27] DHI, «MIKE 3 MT FM, Mud Transport Flexible Mesh, Scientific Documentation,» MIKE by DHI, Hørsholm, 2017.
- [28] A. Feola, I. Lisi, A. Salmeri, F. Venti, A. Pedroncini, M. Gabellini e E. Romano, «Platform of integrated tools to support environmental studies and management of dredging activities,» *Journal of Environmental Management*, vol. 166, pp. 357-373, 2016.
- [29] J. Becker, E. Van Elke, J. Van Wiechen, W. De Lange, T. Damsma, T. Smolders e M. Van Koningsveld, «Estimating source terms for far field dredge plume modelling,» *Journal of Environmental Management*, vol. 149, pp. 282-293, 2015.
- [30] D. Xu, Y. Bai, C. Ji e J. Williams, «Experimental study of the density influence on the incipient motion and erosion modes of muds in unidirectional flows: the case of Huangmaohai Estuary,» Berlino, 2014.
- [31] C. Fischenich e C. Little, «Sediment Sampling and Analysis for Stream Restoration Projects,» 2007.
- [32] Autorità Portuale di Trieste, «Studio Ambientale Integrato - Quadro di Riferimento Progettuale,» in *Piano Regolatore Portuale del Porto di Trieste*, Luglio 2013.
- [33] Istituto Idrografico della Marina di Genova, «Carta batimorfologica dell'Adriatico Settentrionale,» in *Progetto Bandiera RITMARE (La Ricerca Italiana per il Mare), Programma Nazionale della Ricerca finanziato dal Ministero dell'Istruzione, dell'Università e della Ricerca*, Dicembre 2017.

General description of the models' chain

The models and datasets used for the development of the MWM database are:

- the *CFSR (Climate Forecast System Reanalysis)* global re-analysis dataset, produced and freely published by NCEP (*National Centers for Environmental Prediction*) (Saha et al, 2010; <http://rda.ucar.edu/datasets/ds093.0/index.html#description>), hourly (re-forecast) data with a space resolution of 0.5°; these data are used as initial (IC) and boundary conditions (BC) of the *WRF-ARW model* (below);
- the atmospheric model *WRF-ARW – version 3.4.1 (Weather Research and Forecast - Advanced Research WRF)*, model developed by NCAR (*National Center for Atmospheric Research*) (Skamarock and Klemp, 2007; Michalakes et al, 2001; Michalakes et al, 2005); *WRF-ARW* is presently considered among the best state-of-the-art non-hydrostatic meteorological models; it is supported by a massive worldwide community that contributes to its local use and development (<http://www.mmm.ucar.edu/wrf/OnLineTutorial/index.htm>; <http://www.wrf-model.org/index.php>);
- the wave model *MIKE 21 Spectral Waves (SW)* developed by DHI (former Danish Hydraulic Institute) (Sorensen, O.R., Kofoed-Hansen, H., Rugbjerg, M. and Sorensen, L.S., 2004). *MIKE 21 SW* is among the state of the art wave models, widely used in thousands of offshore and coastal applications worldwide.

In the following a description of the *CFSR* dataset, the *WRF-ARW* and the *MIKE 21 SW* model is given, with specific interest to the implementation adopted in MWM.

CFSR Dataset

The *CFSR* dataset (Fig. A.1) is the result of a long and complex process performed by NCEP, an ensemble of nine weather prediction centers in the United States belonging to the *NWS (National Weather Service)* of the *NOAA (National Oceanic and Atmospheric Administration)*. The simulation, completed in 2011, is based on a global atmospheric numerical model including atmosphere-ocean and sea-ice couplings, with a systematic ingestion of both conventional (point) and satellite observations with data assimilation procedures.

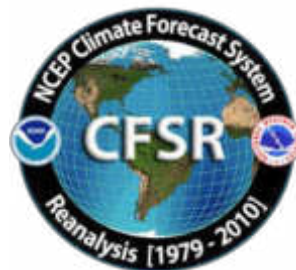


Figure A.1

The *CFSR* now covers a 35-year period from 1979 to 2013 (included) and is continuously updated with new recent data. The simulations were performed as 9 hours forecast simulations, initialized 4 times a day (at 00:00, 06:00, 12:00 and 18:00) between the 6-hourly re-analysis frames. The

results of these simulations, gathered in the CFSR dataset, consist in complete atmospheric data over ocean and lands with a one hour time resolution and a 0.5° horizontal resolution, while the vertical resolution changes greatly amongst the atmospheric variables, spanning from the single surface value up to values at 64 different isobaric levels.

MWM dataset ingest the 6-hourly CFSR data, specifically the *ds093.0* dataset.

Chawla et al (2013) presented a thorough analysis of the *CFSR* dataset against satellite and oceanic buoys data. The final goal of that study is the use of the U_{10} wind data from the *CFSR* dataset as the forcing term of *WWIII* to generate wave fields at global scale, without any assimilation of wave data. The analysis of the *CFSR* dataset shown in that paper includes the intrinsic performance of the model in terms of the seasonal and annual variability of the percentiles. A moving average is applied to smooth the altimeter data from the satellites and from the buoys. The normalized percentiles ("...normalized with the wind speeds at corresponding percentiles from the altimeters") computed over the satellite tracks exhibit an oscillatory behavior, never below 0.93 or 0.90 in the Northern and Southern hemisphere respectively. From that analysis, the wind and wave *CFSR* and *WWIII* data compare very well with satellite data in terms of normalized percentiles. The Q-Q plots at selected offshore buoys are generally good or very good, with some unexpected variations from case to case for some buoys close to the coast, with even a contradictory behavior between U_{10} and H_s in some locations.

The analysis of the wind field of the *CFSR* dataset is far beyond the scope of the present work but still some checks have been done in specific cases, like the event of November 1999 in Trieste (Italy). The performance of a local area model is directly related to the information contained in the global model used as boundary and initial conditions; Fig. A.2 after Contento et al (2014) shows the wind speed for the case of November 1999 in Trieste (Northern Adriatic Sea - Italy); the red dots are experimental data by NOAA (<http://gis.ncdc.noaa.gov/map/viewer/#app=cdo&cfg=cdo&theme=hourly&layers=1&node=gis>); the yellow line corresponds to the re-analysis data *CFSR d093.0* (Saha et al, 2010; <http://rda.ucar.edu/datasets/ds093.0/index.html#description>) interpolated at the same position of the station; the blue dots are related to a fully certified and verified measurement station of the Regional Agency for the Environment Protection (ARPA FVG-OSMER, <http://www.osmer.fvg.it/home.php>) located few meters far from the station used by NOAA (<http://gis.ncdc.noaa.gov/map/viewer/#app=cdo&cfg=cdo&theme=hourly&layers=1&node=gis>); the cyan line corresponds to the present hindcast dataset (model *WRF-ARW*). It is rather evident that the *CFSR* dataset ingests the experimental data from NOAA but there are some non-negligible discrepancies between the two experimental datasets (private communication with ARPA FVG-OSMER - Regional Agency for the Environment Protection – Friuli Venezia Giulia Region, Italy). In this case the local model *WRF-ARW* is able to develop the local wind field and matches correctly the measurement by ARPA, irrespective of the wrong assimilated data as BC and IC; this, however, cannot be always guaranteed.

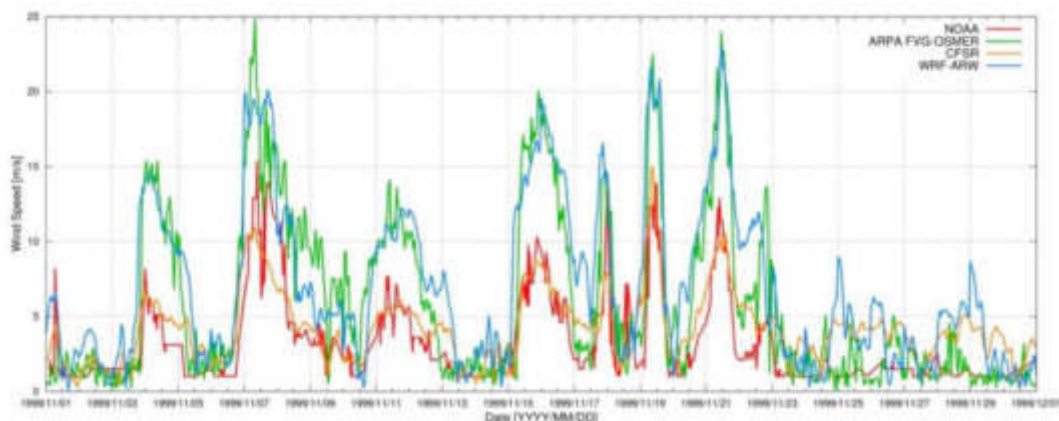


Figure A.2 Comparison between measured wind speed at two ground neighbor (few meters from each other) stations in Trieste (Italy - Northern Adriatic Sea) from the database of NOAA

(<http://gis.ncdc.noaa.gov/map/viewer/#app=cdo&cfg=cdo&theme=hourly&layers=1&node=gis>) (red line) and from ARPA-FVG OSMER (<http://www.osmer.fvg.it/home.php>) (blue line). Model data from CFSR (Saha et al, 2010) (yellow line) and the present simulations with WRF-ARW (cyan line) are overlapped.

The scope of these checks was solely to verify the sensitivity of the CFSR wind pattern to a complex steep geographic area facing the sea. The eastern coast of the Adriatic Sea is just an example among many others. The availability of certified wind data from the local Regional Agency for the Environment Protection – Friuli Venezia Giulia (ARPA FVG-OSMER, <http://www.osmer.fvg.it/home.php>) related to ground stations and to a fixed station in the middle of the Gulf of Trieste (Northern Adriatic Sea <http://www.ts.ismar.cnr.it/node/84>), helped a lot in defining the set-up of the local area meteorological model. The aim of the set-up process was to let the model WRF-ARW develop mesoscale and local weather structures, thus using a domain large enough to develop these structures, but at the same time avoiding the use of too large a domain that may lead to a model drift from the experimental data. These undesired effects were observed along the entire Adriatic Sea, specifically on the eastern side (Contento et al, 2011; Contento et al, 2014).

WRF-ARW meteorological model

The WRF model is an open source mesoscale to microscale atmospheric model developed by the American atmospheric research center NCAR in cooperation with many other meteorological institutions. It is largely used worldwide for both atmospheric research and forecast or hindcast purposes due to its ability to perform atmospheric simulations over a wide range of length scales spanning from less than 1 kilometer to thousands of kilometers. This flexibility is further increased by its capability of performing two way coupled nested runs.

The WRF modelling system includes a pre-processor system (WPS), a data assimilation system (WRF-DA) and the dynamic solver. During this work the ARW dynamic solver, developed and maintained by the Mesoscale and Microscale Meteorology Division of NCAR, has been used. The ARW dynamic core is a fully compressible and non-hydrostatic model, based on a terrain-following hydrostatic pressure vertical coordinate system and on an Arakawa C-grid staggered evaluation of the vector quantities. The solver uses high order time integration and 3-D advection schemes.

The WRF model works internally with NetCDF files, a self-describing and machine-independent data format particularly suitable for the manipulation of long arrays of scientific data.

A WRF-ARW model run is a quite complex process, since it involves several different steps to be run in a precise order. First of all, WRF requires boundary and initial conditions; these conditions can be supplied by the GRIB files obtained from the CFSR dataset files described in CISL RDA: NCEP Climate Forecast System Re-analysis (CFSR) 6-hourly Products, January 1979 to December 2010.” [Online] Available at <http://rda.ucar.edu/datasets/ds093.0/index.html#description>

GRIB files needed to cover completely the whole simulated period must be fed to the model to complete the simulation process successfully.

Moreover, since the atmosphere behaviour is strongly dependent on the soil characteristics, detailed data about these characteristics must be fed to the model too in order to let it develop the local weather phenomena correctly. However, there is no need to produce this type of data since suitable 30" resolved geographic data are included in the default WRF pre-processing (WPS). Since these data are time-independent they need to be downloaded only once, and they remain valid for every simulation unlike the GRIB files. Actually, some of the parameters contained in the geographic data cannot be considered as completely time-independent; in fact, some of the parameters show a time dependence which, however, is limited to seasonal changes, e.g. the

reduced vegetation cover in winter. The possible seasonal variability of the geographical parameters is included in the geographical data archive of WPS.

A complete WRF-ARW simulation needs the WPS (*WRF Pre-processor System*) to be run before the numerical solver (*wrf.exe*). The WPS pre-processor system deals with both the domain set-up and the preliminary input manipulations; it is composed by three main executables carrying out different tasks:

- *geogrid.exe* is responsible for the definition of the horizontal grid as well as for the interpolation of the geographic data on the user-defined grid. When performing nested runs, the *geogrid.exe* run produces a NetCDF file *geo_em.dxx.nc* containing the grid and geographic data for each domain, where *xx* stands for the code of the domain (01, 02, ...).
- *ungrib.exe* is responsible for the decoding of the input GRIB files used as initial and boundary conditions. The GRIB files, which need to be linked to the work directory of WPS by means of the script *link_grib.csh*, are “ungribbed” and rewritten in an intermediate format suitable for further manipulations, excluding all the fields not needed for the following model run.
- *metgrid.exe* is responsible for the horizontal interpolation of the intermediate input files produced by *ungrib.exe* on the grid defined by *geogrid.exe*. Moreover, the geographic data contained in the *geo_em* files are ingested by *metgrid* and written on its output files. The output of *metgrid.exe* is in fact composed by the NetCDF files *met_em.dxx.YYYY-MM-DD_HH:00:00.nc*, each containing the interpolated boundary conditions and geographic data for the *xx* domain and for every timestep of the supplied GRIB files. In the case considered, as the CFSR dataset is composed of hourly data, the produced *met_em* files are hourly spaced too.

The whole WPS process is controlled by a single external configuration file: *namelist.wps*, which contains the user specified parameters defining the time length and the domain of the simulation as well as the time and space resolutions.

An additional manipulation is needed before launching the actual solver: the NetCDF data produced by *metgrid.exe* must be vertically interpolated onto the user-defined vertical levels of the WRF simulation. This task is performed by the *real.exe* executable, which, despite actually being a pre-processing routine, is not included in the WPS system. The *real.exe* run finally produces the NetCDF files needed by the bare solver: *wrfinput_dxx* and *wrfbdy_dxx*, containing respectively, for each of the nested domains under simulation, the initial condition inclusive of the domain geographic data and the boundary conditions forcing the domain over time.

The last step of a WRF-ARW model simulation is the *wrf.exe* solver run which performs the numerical integration and produces the final output files *wrfout_dxx.YYYY-MM-DD_HH:MN:SS*, one for each simulated domain and for every temporal frame in the total simulated period. Each *wrfout* file contains therefore the complete atmospheric variables set calculated by the ARW solver for every point of the user defined simulation 3-D grid at a single temporal frame.

Both *real.exe* and *wrf.exe* are controlled by *namelist.input*, an external configuration file gathering the user defined parameters regarding the vertical resolution of the simulation, the atmosphere microphysical parameters and, again, the time / length scales and resolutions of the simulation.

A script that makes all steps involved automatic in a WRF-ARW simulation procedure, from the set-up of the configuration files to the archiving of output files, was developed and tested extensively.

The above depicted working scheme is summarized in Figure A.3:

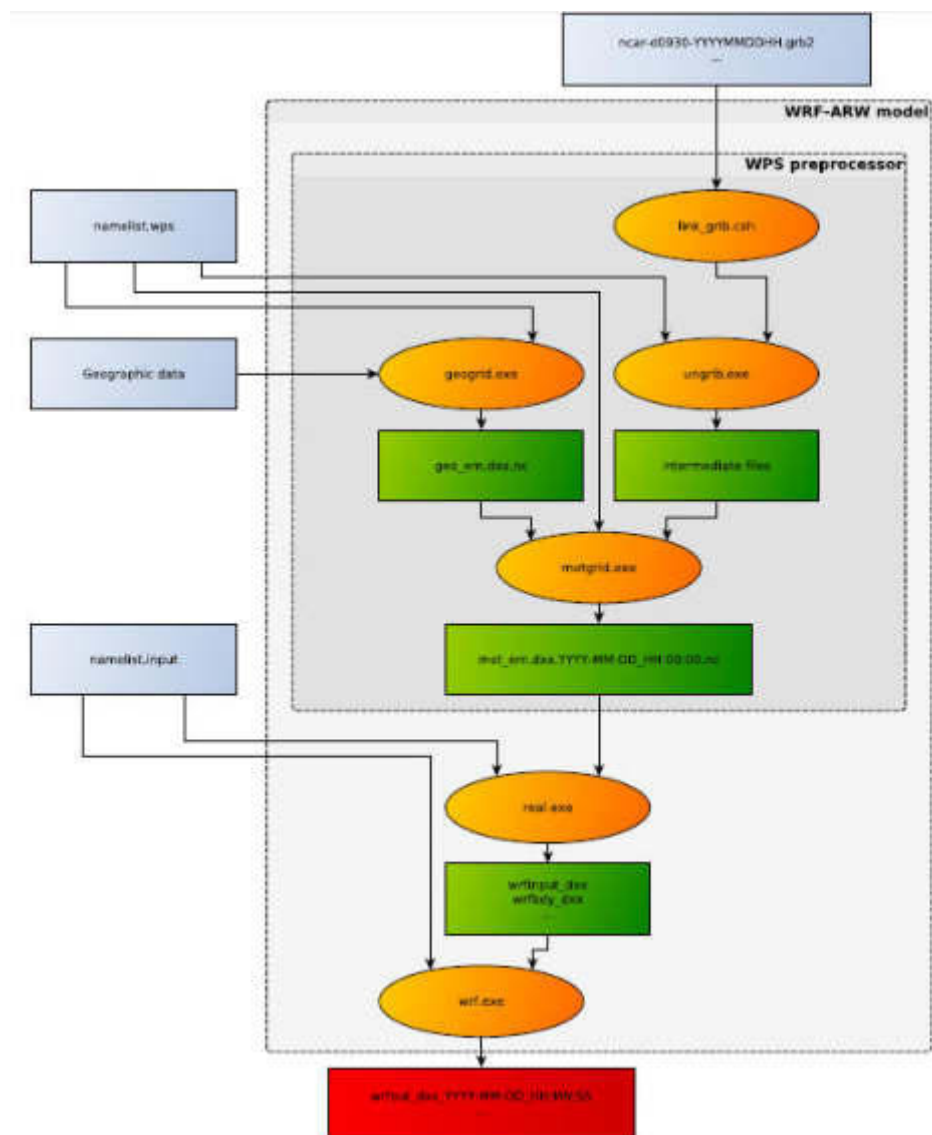


Figure A.3 Working scheme of the WRF-ARW model.

WRF-ARW domains, resolution, set-up in MWM

The preliminary set-up and tuning of the met-ocean models chain was performed simulating the month of November 1999, chosen for the remarkable number of very intense storms occurred over the Mediterranean Sea. The second step, before running the entire period 1979-2013, was done simulating one complete year, from November 1999 to October 2000, relying on 41 ground stations along the Mediterranean coast and 25 wave buoys for comparison. The results obtained in these steps are summarized in Contento et al. (2014), Contento et al. (2012-2014) and Donatini (2013).

The two-steps set-up started with the meteorological model *WRF-ARW*, adopting different configurations (domain size, resolution, run length, spin-up time) and comparing the wind speed and direction with observational data from ground stations. Since the *CFSR* (Saha et al, 2010) re-analysis dataset reproduces large scale events correctly, after several tests the final decision was to adopt three relatively small, overlapping domains, which cover respectively the Western, Eastern and Central Mediterranean Sea (Fig. A.4). Hereafter these domains will be referred as MEW, MEE and MEC respectively. The wind field obtained from the 3 domains was merged in a

single dataset by a bi-linear interpolation on a Lat-Lon grid and by a linear blending of the results inside the two overlapping zones (Fig. A.4).

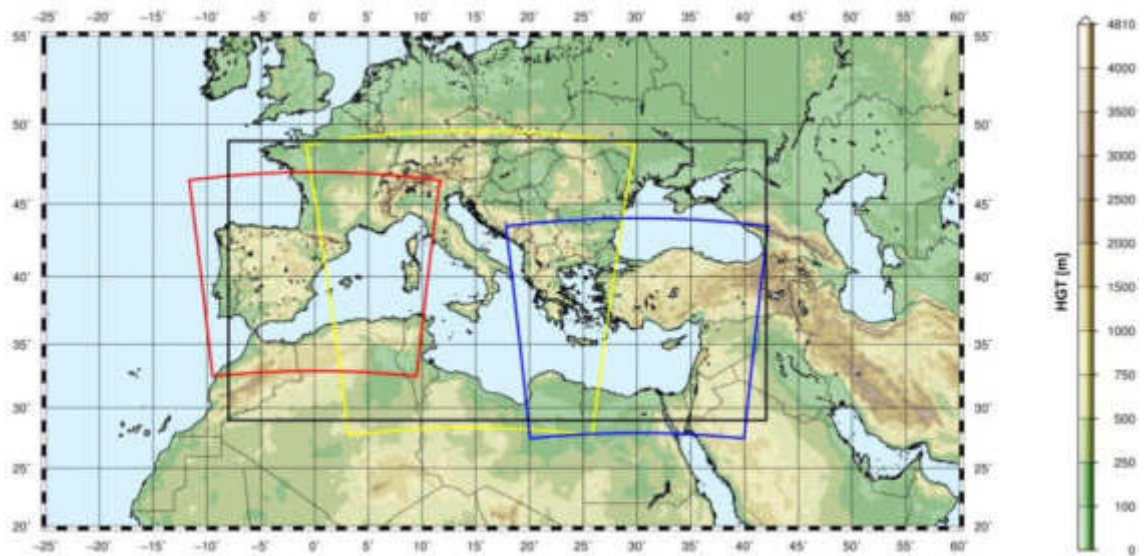


Figure A.4 WRF-ARW domains (red=domain MEW, yellow=domain MEC, blue=domain MEE) and interpolation/blending domain (black line).

The horizontal resolution of *WRF-ARW* was set to 10.53 km, with a grid ratio to the *CFSR* re-analysis data of 1:5 approximately. An additional domain (ITN) with a resolution of 3.51 km was run over Northern Italy as a nested domain of MEC.

The time length of the model run, in terms of hours simulated continuously between two consecutive model initializations with *CFSR* frames, proved to be among the most important parameters that influence the quality of the results. Keeping a small run length reduces the risk of model drift. On the other hand, shortening it excessively may lead to a too constrained behavior of the model, which prevents the correct development of the mesoscale weather structures. The problem of the model drift proved to be particularly tough over the Adriatic Sea where the orography is rather complex and the North-Eastern wind (Bora) can occasionally reach the speed of 150 km/h or more in very narrow zones.

A spin-up time window was used in order to let the model *WRF-ARW* ingest and process the coarser initial conditions from *CFSR*, thus letting it evolve and develop local weather structures. This spin-up window was overlapped with the tail of the previous run so that the data of the simulation during the spin-up window were discarded. The time length of this overlapping window is typically of few hours.

The Mediterranean Sea is a very complex basin from the meteorological point of view, with violent storms usually characterized by a short duration. The two examples given below show the importance of resolving the large space and time gradients of the variables.

Fig. A.5 shows a typical winter wind pattern (from the present simulations, 5 December 2009). The well-known 3 major narrow gates of the “Bora” wind over the Adriatic Sea are well captured by the model, i.e. Trieste (Italy), Rijeka and Sibenik (Croatia). The reference distance of these large variations is of 1° at most.

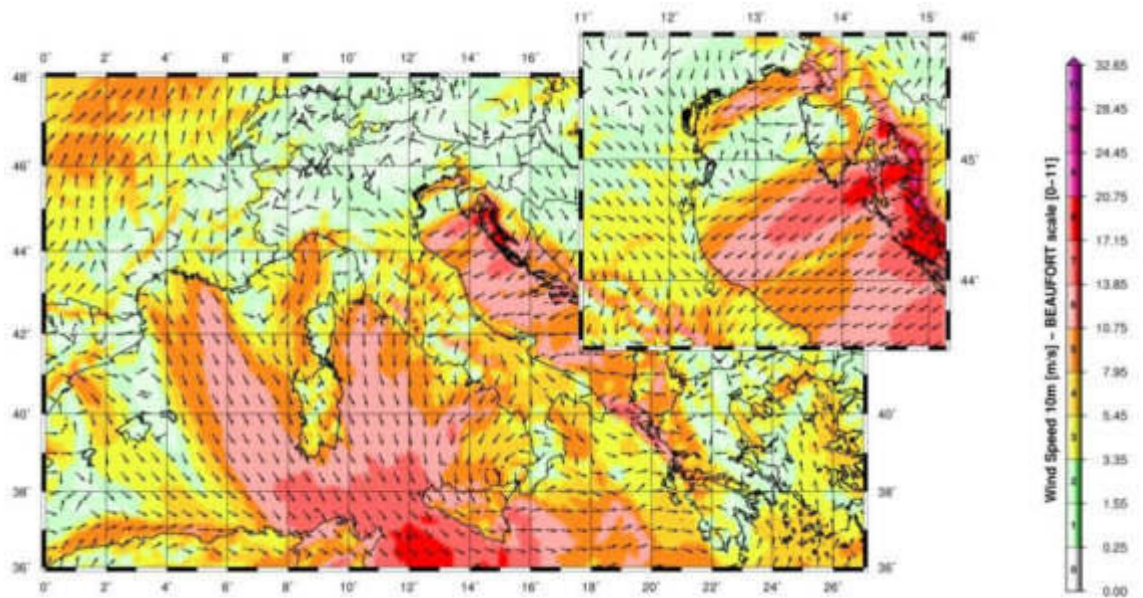


Figure A.5 A typical winter wind pattern over the Mediterranean Sea (from the present simulations, 5 December 2009). The well-known 3 major narrow gates of the “Bora” wind over the Adriatic Sea are well captured by the model, i.e. Trieste (Italy), Rijeka and Sibenik (Croatia). The upper-right figure shows a zoom over the Northern part of the Adriatic Sea (Istria peninsula).

Fig. A.6 (Contento et al., 2011) shows the time series of the wind speed during a squall event occurred on August 2008 in the Gulf of Trieste that caused the loss of two human lives and damages in the main harbor. The squall lasted about 10 min reaching more than 20 m/s from an almost calm situation. The red line corresponds to the results of the operational forecast meteorological model *WRF-ARW* run at that time by some of the authors of this work for ARPA FVG-OSMER, <http://www.osmer.fvg.it/home.php>. The black line corresponds to the measurement at the station PALOMA (45° 37' 06" N, 13° 33' 55" E) [<http://www.ts.ismar.cnr.it/node/84>]. The station is a fixed pole in the middle of the Gulf of Trieste. The measured wind speed is 5 min averaged with 5 min samples. The time step of the model is approximately 13 s. This situation is not uncommon in the Adriatic zone, mostly during the summer, with violent fronts from North and North-West then rotating to North-East.

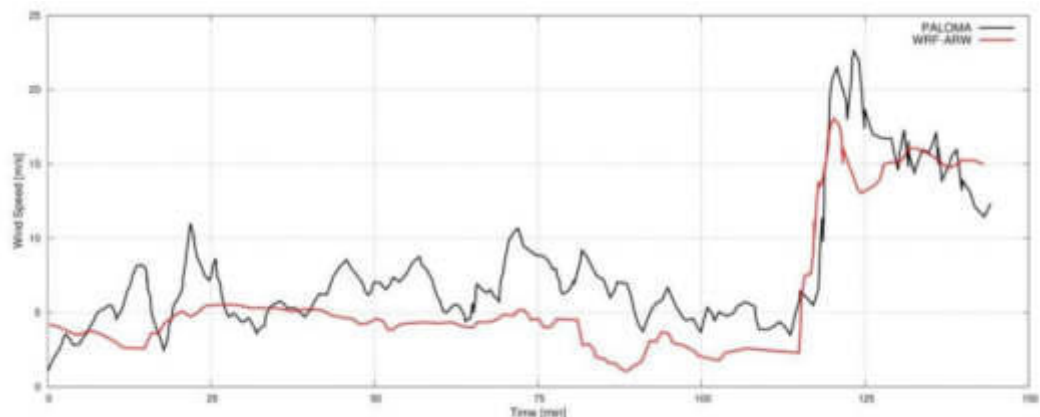


Figure A.6 Time series of the wind speed during a squall event occurred on August 2008 in the Gulf of Trieste. The squall lasts about 10 min reaching over 20 m/s from an almost calm situation. The red line corresponds to the results of the operational forecast meteorological model *WRF-ARW*. The black line corresponds to the measurements at the measurements station PALOMA (45° 37' 06" N, 13° 33' 55" E) [<http://www.ts.ismar.cnr.it/node/84>]. The measured wind speed is 5 min averaged with 5 min samples. The time step of the model is approximately 13 s.

MIKE 21 SW wave model

The wave modeling system includes the state of the art third generation spectral wind-wave model MIKE 21 SW, developed by DHI. MIKE 21 SW simulates the growth, decay and transformation of wind-generated waves and swell in offshore and coastal areas.

MIKE 21 SW includes two different formulations:

- Directional decoupled parametric formulation
- Fully spectral formulation

and includes the following physical phenomena:

- Wave growth by action of wind
- Non-linear wave-wave interaction
- Dissipation due to white-capping
- Dissipation due to bottom friction
- Dissipation due to depth-induced wave breaking
- Refraction and shoaling due to depth variations
- Wave-current interaction
- Effect of time-varying water depth

The discretization of the governing equation in geographical and spectral space is performed using cell-centered finite volume method. In the geographical domain, an unstructured mesh technique is used. The time integration is performed using a fractional step approach where a multisequence explicit method is applied for the propagation of wave action.

For the production of the MWM database, the fully spectral formulation has been adopted, based on the wave action conservation equation, as described in e.g. Komen et al. and Young where the directional-frequency wave action spectrum is the dependent variable.

The time integration of the governing equations is done by using a dynamically determined time step. The time step is determined in order to verify the stability criteria (CFL number).

The only driving force is represented by the two components of wind fields U10 and V10, (x and y component of wind at the elevation of 10m). The process by which the wind transfers energy into the water body for generating waves is controlled by a uncoupled air-sea interaction.

The spectral discretization adopted in the wave model has been deeply investigated and the final configuration is able to guarantee at the same time a high level of accuracy of the results and a reasonable computational effort.

The model domain covers the whole Mediterranean Sea but the spatial resolution is not the same everywhere: while in the offshore areas the spatial resolution is around 0.1° , when approaching the coast the spatial resolution increases up to around 0.03° .

The wave model is forced by the wind fields coming from the WRF Atmospheric models, illustrated above. The wave model generated results in terms of wave parameters (Significant Wave Height, Wave Periods, Wave Directions, etc.) over the whole domain and, in addition, spectral parameters in predefined output locations have been stored, too.

MIKE 21 SW domain, resolution, set-up in MWM

The model domain, covering the entire Mediterranean Sea, is illustrated in Figure A.7.

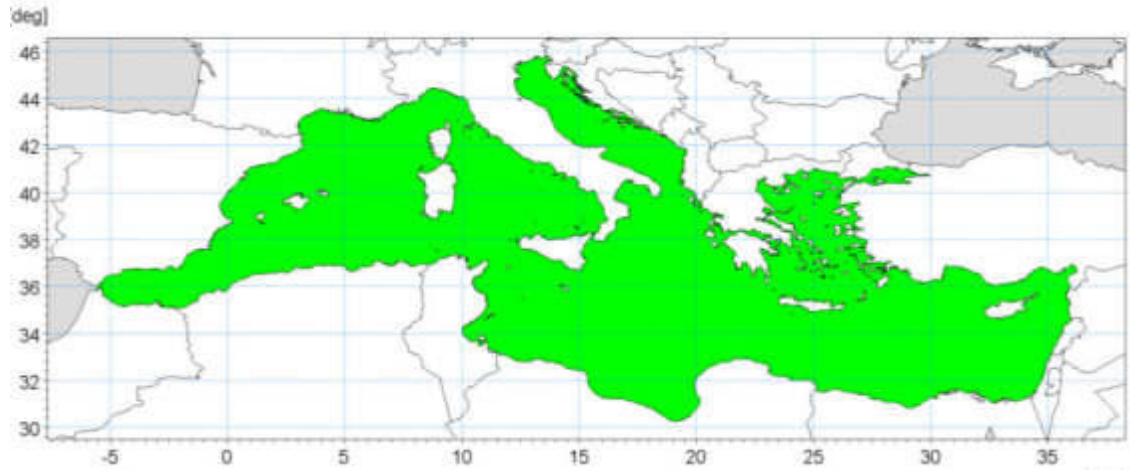


Figure A.7 Wave model domain filled in green

The unstructured mesh, generated over the entire domain by means of a specific tool included in MIKE 21 package, is characterized by different resolutions (in terms of mean length of triangle sides) over the domain. In particular the following criteria have been adopted:

- a coarser resolution of 0.1° (about 10 Km) is used for offshore areas;
- a finer resolution of 0.03° (about 3 Km) has been adopted in shallow water areas, where bathymetry is less than 100m depth or, in coastal areas characterized by very steep profiles, where the distance from the coastline is less than $5\div 10$ Km.

Figure A.8 illustrates the computational mesh of the Mediterranean wave model.

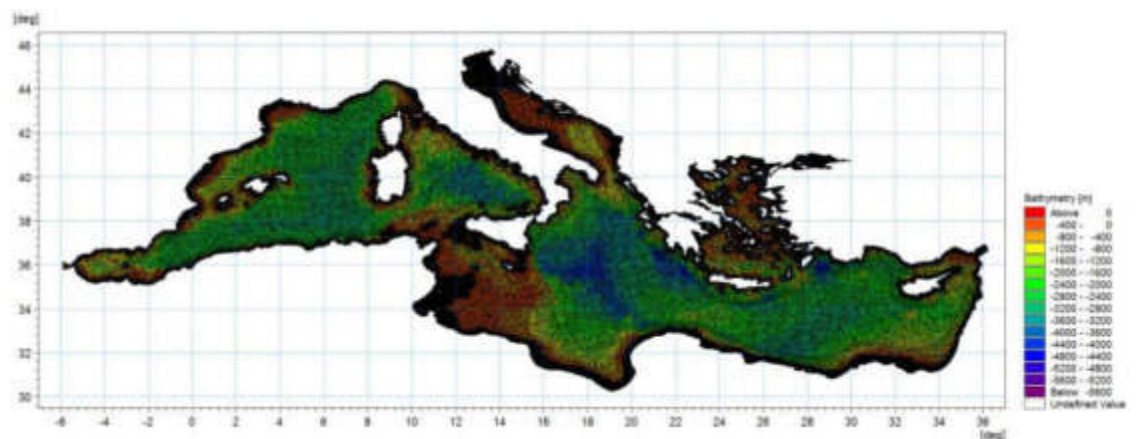


Figure A.8 - Mediterranean wave model computational mesh

Figure A.9 illustrates a detail of the above computational mesh, with special focus on the Adriatic Sea.

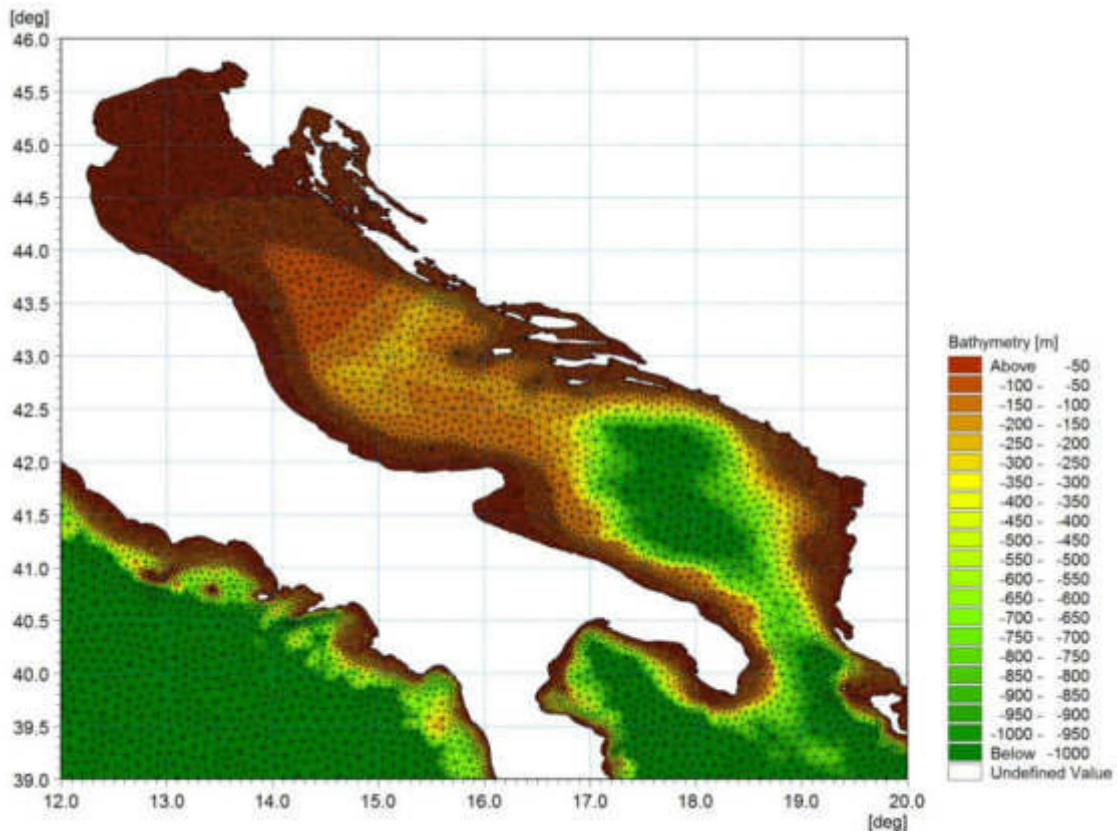


Figure A.9 - Detail of the mesh – Adriatic Sea

Scatter bathymetry data have been derived from GEBCO_08 database. The GEBCO_08 Grid is a 30 arc-second grid of global elevations and it is a continuous terrain model for ocean and land. The grid was generated by combining quality-controlled ship depth soundings with interpolation between sounding points guided by satellite-derived gravity data.

The gridded data are stored in a netCDF data file. Grids are stored as one dimensional arrays of 2-byte signed integer values. The complete data sets provide global coverage. Each data set consists of 21,600 rows x 43,200 columns, resulting in a total of 933,120,000 data points. The data start at the Northwest corner of the file, i.e. for the global file, position 89°59'45"N, 179°59'45"W, and are arranged in latitudinal bands of 360 degrees x 120 points/degree = 43,200 values. The data range eastward from 179°59'45"W to 179°59'45"E. Thus, the first band contains 43,200 values for 89°59'45"N, then followed by a band of 43,200 values at 89°59'15"N and so on at 30 arc-second latitude intervals down to 89°59'45"S. Data values are pixel centred registered, they refer to elevations at the centre of grid cells.

Figure A.10 illustrates GEBCO_08 scatter data for the entire area of the Mediterranean Sea.

GEBCO scatter data have not been used in the whole domain of the Mediterranean Sea. Following a detailed check of agreement and discrepancies between GEBCO database and nautical charts, it has been assumed to limit the use of GEBCO database for offshore areas (up to 500 m water depth) and to use nautical charts for shallower water areas (mainly coastal areas).

The nautical charts database which has been used is the CM93/3 database from CMAP.

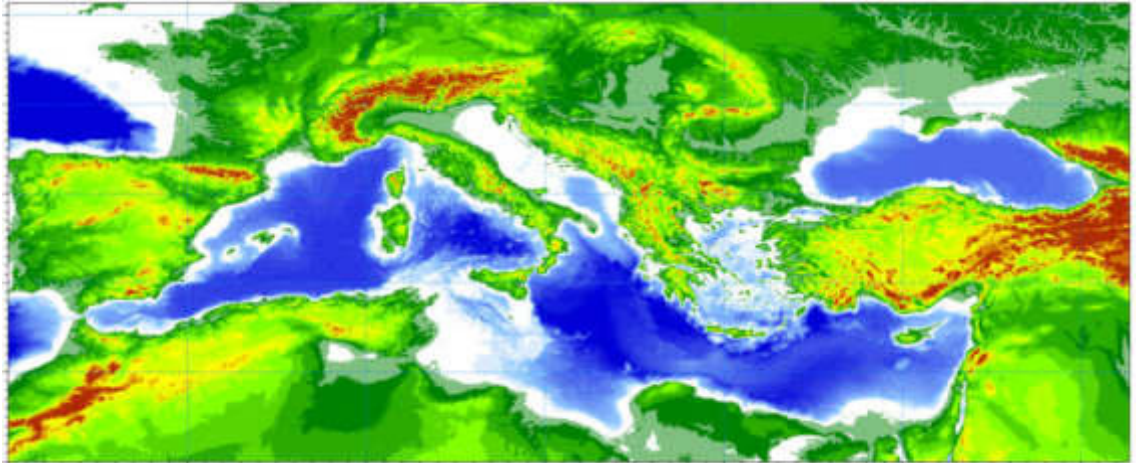


Figure A.10 - Scatter bathymetry data derived from GEBCO_08 database

The number of discrete frequencies and directions form the so called “spectral resolution”, which is a key parameter for wave models in general. The number of discrete frequencies and directions should in fact be high enough to properly represent the “real shape” of the wave spectrum and, on the other hand, it can’t be too high, since it would lead to unacceptable computational times and memory consumption.

In terms of frequency range, the minimum frequency f_{min} (which corresponds to the maximum wave period T_{max} , according to the common relation $f = \frac{1}{T}$) should be able to capture the longest wave periods that can occur in the Mediterranean Sea.

The analysis of ordinary and extreme waves in the Mediterranean Sea (from available data of wave buoys) has highlighted that almost all the wave energy associated to waves in the Mediterranean Sea are associated to wave periods between 1.5 seconds and 20 seconds.

In addition, a logarithmic distribution for the discrete frequencies acts better than a simple linear distribution, since most of the wave periods are concentrated below 8-10 seconds. A number of frequencies around 30 is widely considered as adequate for a proper discretization of wave energy spectra in the Mediterranean Sea. The following formulation has therefore been adopted:

$$f_n = 0.04 \cdot 1.1^n,$$

where n goes from 0 to 29 (30 frequencies in total). The discrete frequencies range from 0.04 Hz to 0.63 Hz (from 1.6s to 25.0s of Mean Wave Period T_m).

Also the choice of the number of discrete directions (directional discretization) is the result of detailed investigations and tests. In particular, a high number of wave model tests, each one characterized by a different spectral resolution (directional), i.e. by a different number of discrete directions have been setup and run.

Few examples of the results of the above model tests are illustrated from Figure A.11 to Figure A.13 in terms of short time series of wave heights extracted at 3 different locations where also measurements were available (La Spezia wave buoy, Ponza wave buoy, Cetraro wave buoy).

In all the below test cases, it appears that the two time series of wave height characterized by 24 and 36 discrete directions are almost coincident. Higher discrepancies can be found for a much limited number of discrete directions (12). After a high number of tests, the 24 directions solution has been assumed as a very good compromise between accuracy of results and computational time (the computational time of the wave model is linearly dependent on the number of discrete directions).

Provided that wave directions can vary within the 360° rose, the directional resolution of the wave model is $360^\circ/24 = 15^\circ$

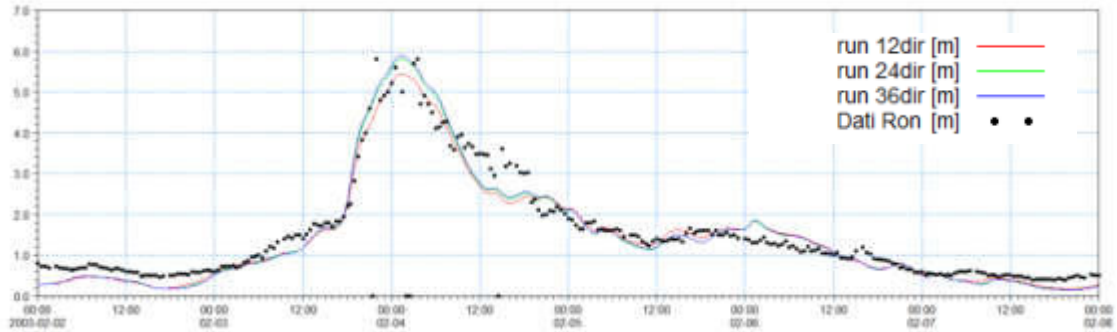


Figure A.11 - Time series of wave height at La Spezia buoy location for 3 different numbers of discrete directions

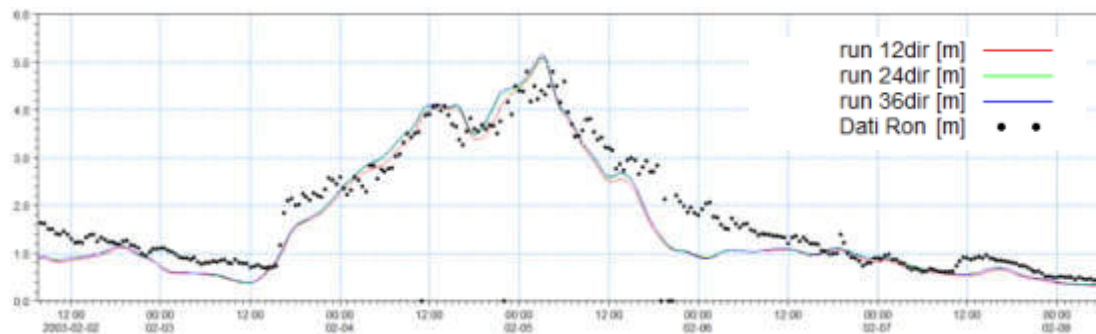


Figure A.12 - Time series of wave height at Ponza buoy location for 3 different numbers of discrete directions

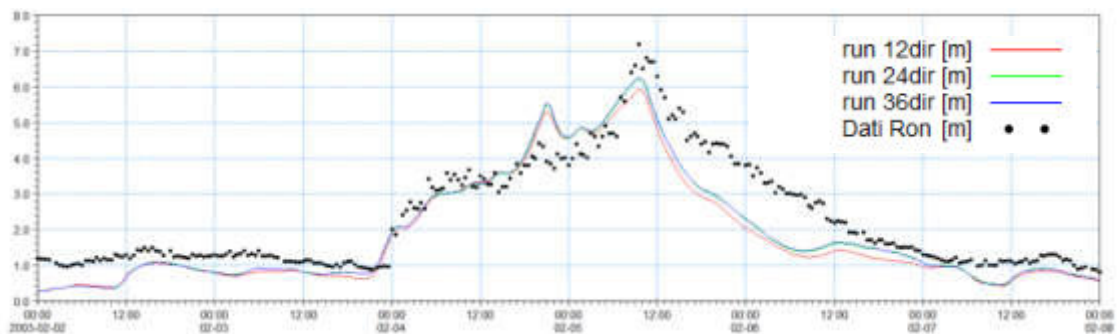


Figure A.13 - Time series of wave height at Cetraro buoy location for 3 different numbers of discrete directions

Available products of the MWM database

The results of the wind and wave model are stored, in the whole domain, in terms of wind parameters and wave parameters averaged over the wave period (“phase averaged results”). In particular, the following hourly time series are available:

- Wind speed, WS [m/s]
- Wind direction, WD [deg]
- Significant Wave height, Hs [m]
- Mean wave period, Tm [s]
- Peak wave period, Tp [s]
- Zero crossing period, Tz [s]
- Mean wave direction, MWD [deg]
- Peak wave direction, PWD [deg]
- Directional standard deviation, DSD [deg]

In addition, hourly spectral results (in terms of wave energy associated to the frequency-direction bins) are saved on a regular grid with an equidistant spatial resolution of 0.1° .

Figure A.14 and Figure A-15 illustrate respectively an example of phase averaged results over a portion of Mediterranean Sea (Hs) and an local example of spectral results.

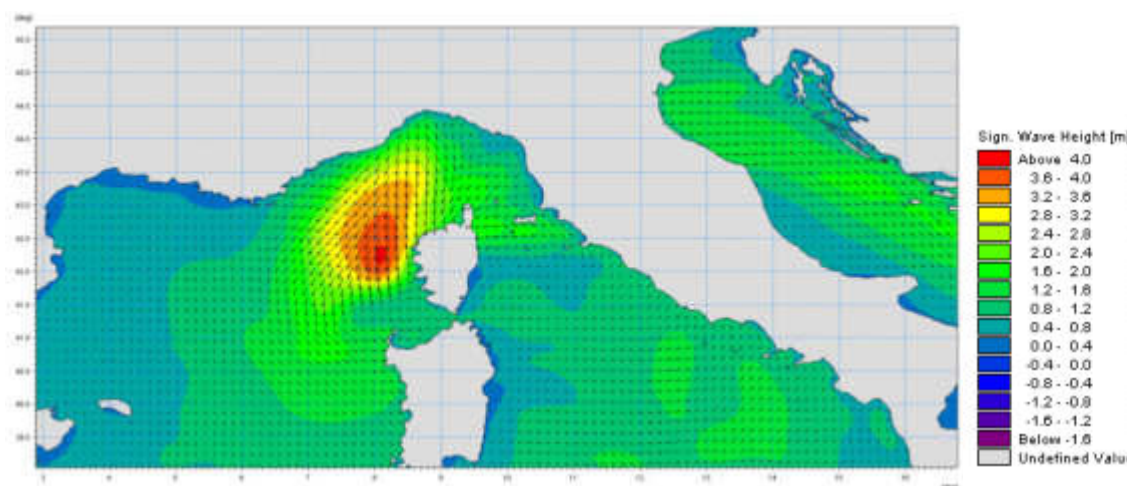


Figure A.14 Phase averaged results: Field of significant wave height and direction

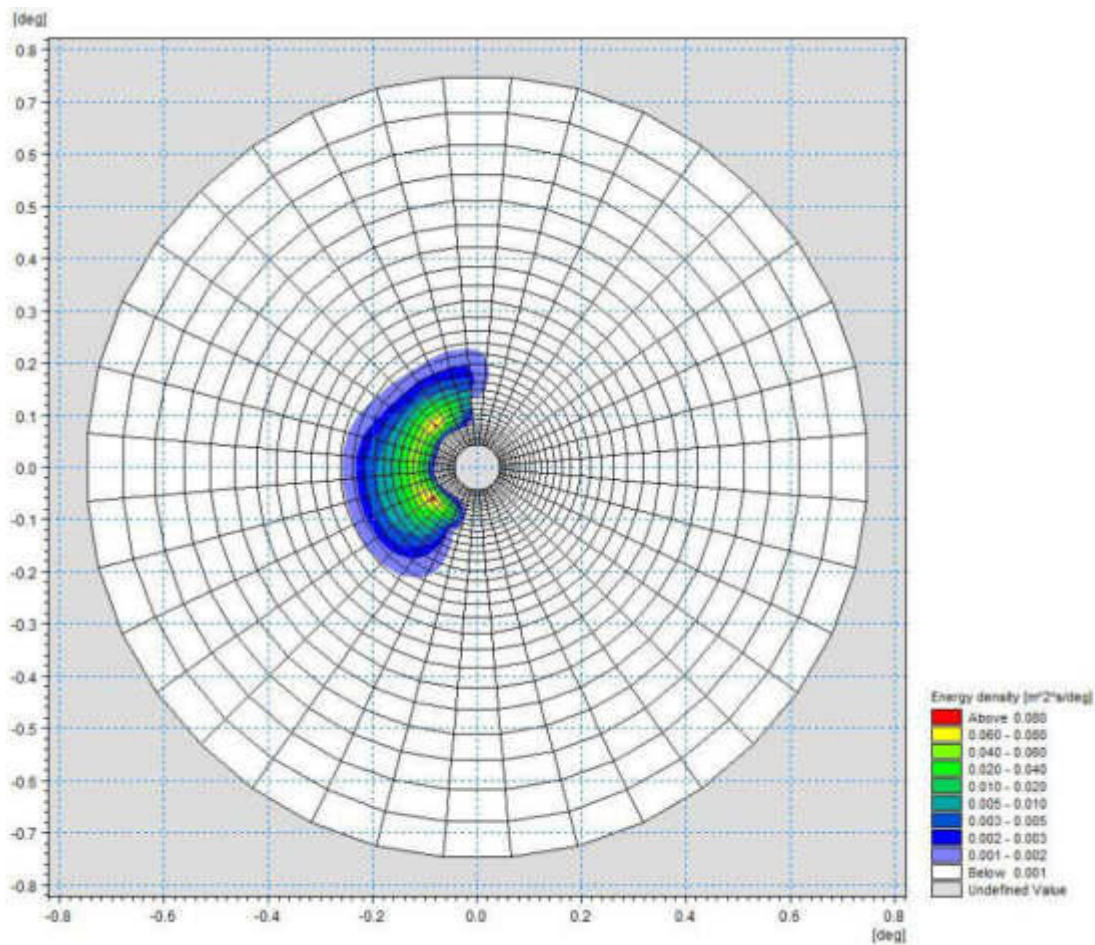


Figure A.15 Polar plot of spectral results. Wave energy density (coloured contours) as a function of directions (angular coordinate) and frequencies (radial coordinate)

References

Arduin, F., Bertotti, L., Bidlot, J.R., Cavaleri, L., Filipetto, V., Lefevre, J.M., Wittmann, P., 2007, Comparison of wind and wave measurements and models in the Western Mediterranean Sea. *Ocean Engineering*, Vol. 34, pp. 526-541.

Athanassoulis, G., Stefanakos, Ch., Cavaleri, L., Ramieri, E., NoEL, C., Lefevre, J.M., Gaillard, P., 2004, RTP 10.10 / WW_MEDATLAS Scientific Report.

Battjes, J.A., Janssen, J.P.F.M., 1978, Energy loss and set-up due to breaking of random waves, Proceedings, 16th Int. Conf. Coastal Eng., ASCE, pp.569-587.

Bolaños-Sanchez, R., Sanchez-Arcilla, A., Cateura, J., 2007, Evaluation of two atmospheric models for wind-wave modeling in the NW Mediterranean. *Journal of Marine Systems* 65:336-353.

Cavaleri, L., Bertotti, L., 2004, Accuracy of the modelled wind and wave fields in enclosed seas. *Tellus*, Vol. 56, pp. 167-175.

Cavaleri, L., 2005, The wind and wave atlas of the Mediterranean Sea – the calibration phase. *Advances in Geosciences*, Vol. 2, pp. 255-257.

Cavaleri, L., Sclavo, M., 2006, The calibration of wind and wave model data in the Mediterranean Sea. *Coastal Engineering*, Vol.53, pp. 613-627.

Chawla, A., Spindler, D.M., Tolman, H.L., 2013, Validation of a thirty year wave hindcast using the Climate Forecast System Reanalysis winds, *Ocean Modelling*, Vol. 70, pp. 189-206.

Contento, G., Lupieri, G., Venturi, M. Ciuffardi, T., 2011, A medium-resolution wave hindcast study over the Central and Western Mediterranean Sea, *Journal of Marine Science and Technology*, Vol. 16(2), pp. 181–201.

Contento, G., Lupieri, G., Donatini, L, Feudale, L, Pedroncini, A., Cusati, L.A., 2014, A state-of-the-art met-ocean model chain for wind&wave hindcast over the Mediterranean and Black Seas: implementation, tuning and validation against field data, accepted for presentation at the 21th Symposium Theory and Practice of Shipbuilding SORTA 2014, Oct. 2-4, 2014, Baška, Island of Krk, Croatia.

Contento, G., Lupieri, G., Donatini, L, 2012-2014, Project SEAPOL - Sistema modellistico ad Elevata risoluzione per l'Analisi storica e la Previsione del moto Ondoso nel mar Ligure, Department of Engineering and Architecture, University of Trieste, Technical Reports codes SEAPOL_UT_1.1.0 to SEAPOL_UT_5.1.0.

Donatini, L., 2013, Implementation of a state-of-art met-ocean model chain for hindcast wave simulations over the Mediterranean Sea and comparison of results with field data, Master Degree Thesis, Department of Engineering and Architecture, University of Trieste, Italy.

Donatini, L., Lupieri, G., Contento, G., 2014, A medium resolution wind&wave hindcast study for the Mediterranean Sea, Journal Paper, under review.

Hasselmann, K., Barnett, T.P., Bouws, E., Carlson, H., Cartwright, D.E., Enke, K., Ewing, J.A., Gienapp, H., Hasselmann, D.E., Krusemann, P., Meerburg, A., Mueller, P., Olbers, D.J., Richter, K., Sell, W., Walden, H., 1973, Measurements of wind-wave growth and swell decay during the Joint North Sea Wave Project (JONSWAP). *Ergaenzungsheft zur Deutschen Hydrographischen Zeitschrift, Reihe, A(8)*, 12, 95 pp.

Hasselmann, S., Hasselmann, K., Allender, J.H., Barnett, T.P., 1985. Computations and parametrizations of the nonlinear energy transfer in a gravity-wave spectrum, Part II: Parametrizations of the nonlinear energy transfer for applications in wave models. *J. Phys. Oceanogr.* Vol. 15, pp. 1378–1391.

ISPRA (formerly APAT), 2004, Agenzia per la Protezione dell'Ambiente e per i servizi Tecnici, Dipartimento Tutela Acque Marine ed Interne, Servizio difesa delle coste, Analisi preliminare dei dati marini lungo le coste italiane – Atlante delle coste – Il moto ondoso al largo delle coste italiane, Technical Report (in Italian). http://www.apat.gov.it/site/_files/Atlante_coste/Introduzione.pdf.

Janssen, P.A.E.M., Abdalla, S., Hersbach, H., Bidlot, J.R., 2007: Error Estimation of Buoy, Satellite, and Model Wave Height Data. *J. Atmos. Oceanic Technol.*, Vol. **24**, pp. 1665–1677. doi: <http://dx.doi.org/10.1175/JTECH2069.1>

Michalakes, J., Chen, S., Dudhia, J., Hart, L., Klemp, J., Middlecoff, J., Skamarock, W., 2001, Development of a Next Generation Regional Weather Research and Forecast Model. *Developments in Teracomputing. In Proceedings of the 9th ECMWF Workshop on the Use of High Performance Computing in Meteorology*. Eds. Walter Zwiefelhofer and Norbert Kreitz. World Scientific, 269-276.

Michalakes, J., Dudhia, J., Gill, D., Henderson, T., Klemp, J., Skamarock, W., Wang, W., 2005, The Weather Research and Forecast Model: Software Architecture and Performance. In *Proceedings of the 11th ECMWF Workshop on the Use of High Performance Computing in Meteorology*. Eds. Walter Zwiefelhofer and George Mozdzyński. World Scientific, 56 - 168.

Ponce del León, S., Guedes Soares, C., 2008, Sensitivity of wave model predictions to wind fields in the Western Mediterranean Sea. *Coastal Engineering*, Vol. 55, pp. 920-929.

Puertos del Estado, Spain, 2009, – (http://www.puertos.es/oceanografia_y_meteorologia/), private communication.

Queffeuou, P., 2004, Long term validation of wave height measurements from altimeters. *Marine Geodesy*, Vol. 27, 495-510.

Queffeuou, P., Croizé-Fillon, D., 2010, Global altimeter SWH data set, version 7, Technical Report, Ifremer, ftp://ftp.ifremer.fr/cersat/products/swath/altimeters/waves/documentation/altimeter_wave_merge__7.0.pdf

Queffeuou, P., 2009, Altimeter Wave Height Measurements - Validation of Long Time Series. Poster: Ocean Surface Topography Science Team meeting, Seattle, Washington, USA. (<http://www.aviso.oceanobs.com/en/courses/ostst/ostst-2009-seattle/posters/>).

Saha, S., Moorthi, S., Pan, H., Wu, X., Wang, J., Nadiga, S., Tripp, P., Kistler, R., Wollen, J., Behringer, D., Liu, H., Stokes, D., Grumbine, R., Gayno, G., Wang, J., Hou, Y., Chuang, H., Juang, H., Sela, J., Iredell, M., Treadon, R., Kleist, D., VanDelst, P., Keyser, D., Derber, J., Ek, M., Meng, J., Wei, H., Yang, R., Lord, S., van den Dool, H., Kumar, A., Wang, W., Long, C., Chelliah, M., Xue, Y., Huang, B., Schemm, J., Ebisuzaki, W., Lin, R., Xie, P., Chen, M., Zhou, S., Higgins, W., Zou, C., Liu, Q., Chen, Y., Han, Y., Cucurull, L., Reynolds, R., Rutledge, G., Goldberg, M., 2010, *The NCEP Climate Forecast System Reanalysis*. *Bull. Amer. Meteor. Soc.*, Vol. 91, 1015–1057.

Skamarock WC, Klemp JB, 2007, A time-split nonhydrostatic atmospheric model for research and NWP applications. *J. Comp. Phys.* Special issue on environmental modeling.

Sorensen, O.R., Kofoed-Hansen, H., Rugbjerg, M. and Sorensen, L.S., 2004: A Third Generation Spectral Wave Model Using an Unstructured Finite Volume Technique. In Proceedings of the 29th International Conference of Coastal Engineering, 19-24 September 2004, Lisbon, Portugal.

Tolman, H.L., 2002a. Alleviating the garden sprinkler effect in wind wave models. *Ocean Modelling*, Vol. 4, pp. 269–289.

Tolman, H.L., 2002f, Validation of WAVEWATCH III, version 1.15 for a global domain. Tech. Note 213, NOAA/NWS/NCEP/OMB, 33p.

Tolman, H.L., 2008, http://cioss.coas.oregonstate.edu/CIOSS/workshops/Altimeter_workshop_08/Coastal_Alt_Presentations/18_Tolman_Sig_Wave_Ht.pdf

Sorensen, O.R., Kofoed-Hansen, H., Rugbjerg, M. and Sorensen, L.S., 2004: A Third Generation Spectral Wave Model Using an Unstructured Finite Volume Technique. In Proceedings of the 29th International Conference of Coastal Engineering, 19-24 September 2004, Lisbon, Portugal.

Komen, G.J., Cavaleri, L., Doneland, M., Hasselmann, K., Hasselmann, S. and Janssen, P.A.E.M., (1984). Dynamics and modelling of ocean waves. Cambridge University Press, UK, 560 pp.

Young, I.R., (1999). Wind generated ocean waves, in Elsevier Ocean Engineering Book Series, Volume 2, Eds. R. Bhattacharyya and M.E. McCormick, Elsevier.

WAMDI-group: S. Hasselmann, K. Hasselmann, E. Bauer, P.A.E.M. Janssen, G.J. Komen, L. Bertotti, P. Lionello, A. Guillaume, V.C. Cardone, J.A. Greenwood, M. Reistad, L. Zambresky and J.A. Ewing, (1988) "The WAM model – a third generation ocean wave prediction model", *J. Phys. Oceanogr.*, 18, 1775-1810

General Bathymetric Chart of the Oceans (GEBCO) – www.gebco.net

CM-93 Edition 3.0, CM-93/3 - www.jeppesen.com/marine/commercial/professional/

Ole Baltazar Andersen (1995), Global ocean tides from ERS 1 and TOPEX/POSEIDON altimetry, J. of Geophys. Res., 100, C12, p. 25249-25260

Doodson, A. T., Warburg, H. D., 1941 "Admiralty manual of tides"

Web references

ARPA-FVG OSMER, [Online] <http://www.osmer.fvg.it/home.php>

ARW Online Tutorial." [Online] Available at <http://www.mmm.ucar.edu/wrf/OnLineTutorial/index.htm>

CISL RDA: NCEP Climate Forecast System Re-analysis (CFSR) 6-hourly Products, January 1979 to December 2010." [Online] Available at <http://rda.ucar.edu/datasets/ds093.0/index.html#description>

NOAA, Hourly/Sub-Hourly Observational Data." [Online] Available at <http://gis.ncdc.noaa.gov/map/viewer/#app=cdo&cfg=cdo&theme=hourly&layers=1&node=gis>

The Weather Research&Forecasting Model Website." [Online] Available at <http://www.wrf-model.org/index.php>



MIKE 21 Wave Modelling

MIKE 21 Spectral Waves FM

Short Description



DHI headquarters

Agern Allé 5
DK-2970 Hørsholm
Denmark

+45 4516 9200 Telephone
+45 4516 9333 Support
+45 4516 9292 Telefax

mike@dhigroup.com
www.mikepoweredbydhi.com

MIKE 21 SW - SPECTRAL WAVE MODEL FM

MIKE 21 SW is a state-of-the-art third generation spectral wind-wave model developed by DHI. The model simulates the growth, decay and transformation of wind-generated waves and swells in offshore and coastal areas.

MIKE 21 SW includes two different formulations:

- Fully spectral formulation
- Directional decoupled parametric formulation

The fully spectral formulation is based on the wave action conservation equation, as described in e.g. Komen et al (1994) and Young (1999). The directional decoupled parametric formulation is based on a parameterisation of the wave action conservation equation. The parameterisation is made in the frequency domain by introducing the zeroth and first moment of the wave action spectrum. The basic conservation equations are formulated in either Cartesian co-ordinates for small-scale applications and polar spherical co-ordinates for large-scale applications.

The fully spectral model includes the following physical phenomena:

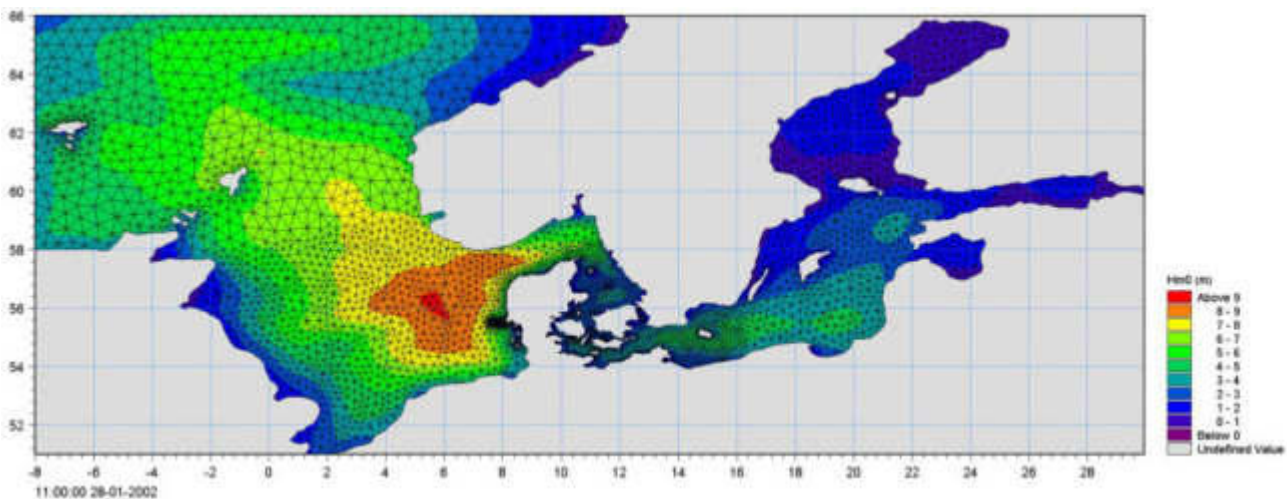
- Wave growth by action of wind
- Non-linear wave-wave interaction
- Dissipation due to white-capping
- Dissipation due to bottom friction

- Dissipation due to depth-induced wave breaking
- Refraction and shoaling due to depth variations
- Wave-current interaction
- Effect of time-varying water depth
- Effect of ice coverage on the wave field

The discretisation of the governing equation in geographical and spectral space is performed using cell-centred finite volume method. In the geographical domain, an unstructured mesh technique is used. The time integration is performed using a fractional step approach where a multi-sequence explicit method is applied for the propagation of wave action.



MIKE 21 SW is a state-of-the-art numerical modelling tool for prediction and analysis of wave climates in offshore and coastal areas. © BIOFOTO/Klaus K. Bentzen



A MIKE 21 SW forecast application in the North Sea and Baltic Sea. The chart shows a wave field (from the NSBS model) illustrated by the significant wave height in top of the computational mesh. See also www.waterforecast.com

Computational Features

The main computational features of MIKE 21 SW - Spectral Wave Model FM are as follows:

- Fully spectral and directionally decoupled parametric formulations
- Source functions based on state-of-the-art 3rd generation formulations
- Instationary and quasi-stationary solutions
- Optimal degree of flexibility in describing bathymetry and ambient flow conditions using depth-adaptive and boundary-fitted unstructured mesh
- Coupling with hydrodynamic flow model for modelling of wave-current interaction and time-varying water depth
- Flooding and drying in connection with time-varying water depths
- Cell-centred finite volume technique
- Fractional step time-integration with an multi-sequence explicit method for the propagation
- Extensive range of model output parameters (wave, swell, air-sea interaction parameters, radiation stress tensor, spectra, etc.)

Application Areas

MIKE 21 SW is used for the assessment of wave climates in offshore and coastal areas - in hindcast and forecast mode.

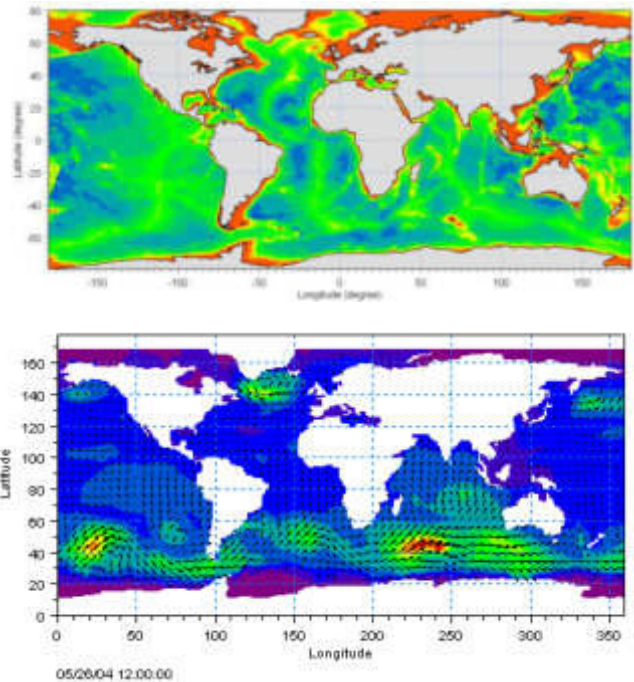
A major application area is the design of offshore, coastal and port structures where accurate assessment of wave loads is of utmost importance to the safe and economic design of these structures.



Illustrations of typical application areas of DHI's MIKE 21 SW – Spectral Wave Model FM

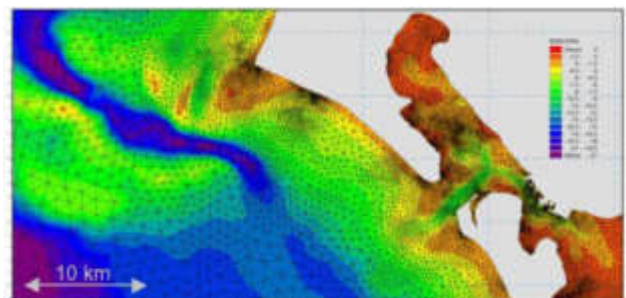
Measured data are often not available during periods long enough to allow for the establishment of sufficiently accurate estimates of extreme sea states.

In this case, the measured data can then be supplemented with hindcast data through the simulation of wave conditions during historical storms using MIKE 21 SW.



Example of a global application of MIKE 21 SW. The upper panel shows the bathymetry. Results from such a model (cf. lower panel) can be used as boundary conditions for regional scale forecast or hindcast models. See <http://www.waterforecast.com> for more details on regional and global modelling

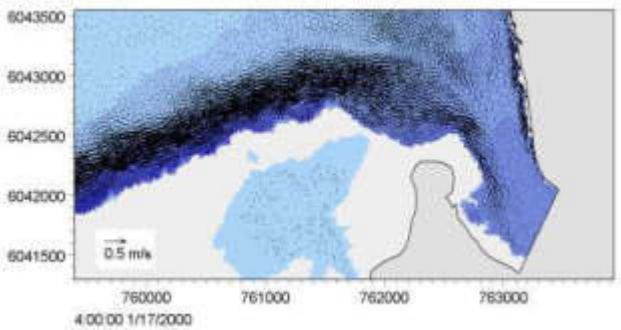
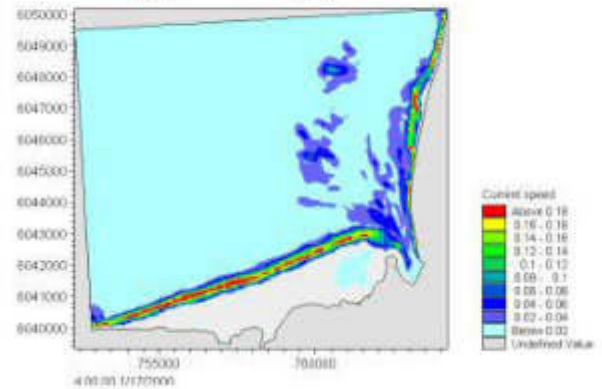
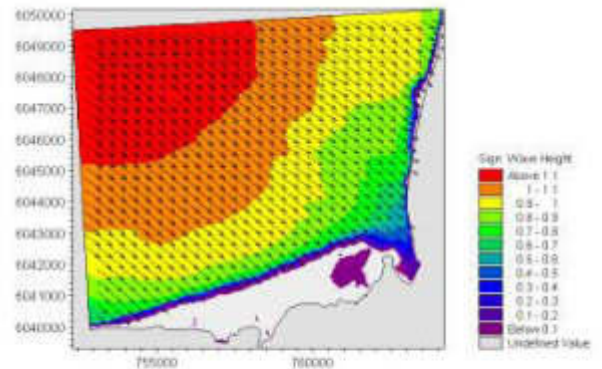
MIKE 21 SW is particularly applicable for simultaneous wave prediction and analysis on regional scale and local scale. Coarse spatial and temporal resolution is used for the regional part of the mesh and a high-resolution boundary and depth-adaptive mesh is describing the shallow water environment at the coastline.



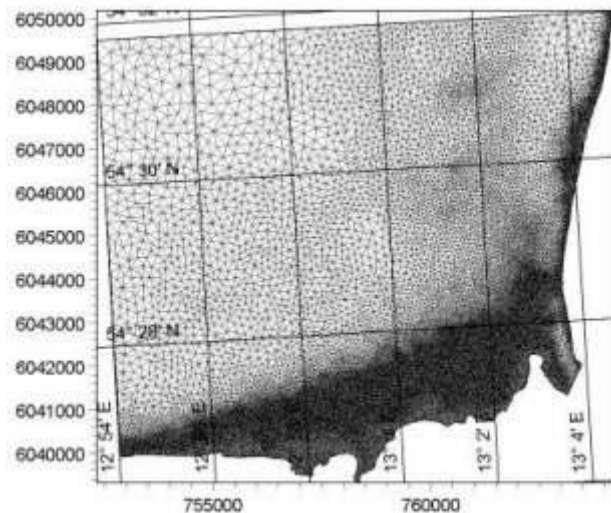
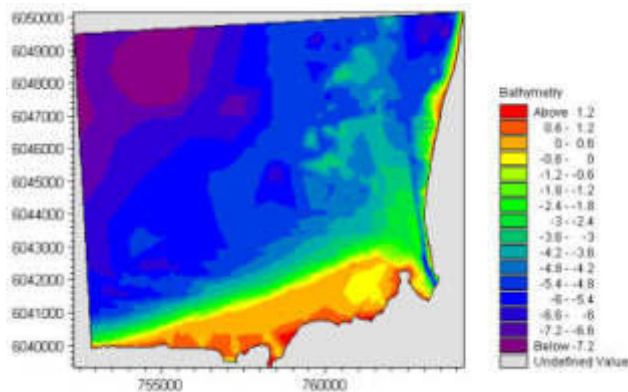
Example of a computational mesh used for transformation of offshore wave statistics using the directionally decoupled parametric formulation

MIKE 21 SW is also used for the calculation of the sediment transport, which for a large part is determined by wave conditions and associated wave-induced currents. The wave-induced current is generated by the gradients in radiation stresses that occur in the surf zone.

MIKE 21 SW can be used to calculate the wave conditions and associated radiation stresses. The long-shore currents and sediment transport are then calculated using the flow and sediment transport models available in the MIKE 21 package. For such type of applications, the directional decoupled parametric formulation of MIKE 21 SW is an excellent compromise between the computational effort and accuracy.



Map of significant wave height (upper), current field (middle) and vector field (lower). The flow field is simulated by DHI's MIKE 21 Flow Model FM, which is dynamically coupled to MIKE 21 SW



Bathymetry (upper) and computational mesh (lower) used in a MIKE 21 SW application on wave induced currents in Gellen Bay, Germany

Model Equations

In MIKE 21 SW, the wind waves are represented by the wave action density spectrum $N(\sigma, \theta)$. The independent phase parameters have been chosen as the relative (intrinsic) angular frequency, $\sigma = 2\pi f$ and the direction of wave propagation, θ . The relation between the relative angular frequency and the absolute angular frequency, ω , is given by the linear dispersion relationship

$$\sigma = \sqrt{gk \tanh(kd)} = \omega - \bar{k} \cdot \bar{U}$$

where g is the acceleration of gravity, d is the water depth and \bar{U} is the current velocity vector and \bar{k} is the wave number vector with magnitude k and direction θ . The action density, $N(\sigma, \theta)$, is related to the energy density $E(\sigma, \theta)$ by

$$N = \frac{E}{\sigma}$$

Fully Spectral Formulation

The governing equation in MIKE 21 SW is the wave action balance equation formulated in either Cartesian or spherical co-ordinates. In horizontal Cartesian co-ordinates, the conservation equation for wave action reads

$$\frac{\partial N}{\partial t} + \nabla \cdot (\bar{v}N) = \frac{S}{\sigma}$$

where $N(\bar{x}, \sigma, \theta, t)$ is the action density, t is the time, $\bar{x} = (x, y)$ is the Cartesian co-ordinates, $\bar{v} = (c_x, c_y, c_\sigma, c_\theta)$ is the propagation velocity of a wave group in the four-dimensional phase space \bar{x} , σ and θ . S is the source term for energy balance equation. ∇ is the four-dimensional differential operator in the \bar{x} , σ , θ -space. The characteristic propagation speeds are given by the linear kinematic relationships

$$(c_x, c_y) = \frac{d\bar{x}}{dt} = \bar{c}_g + \bar{U} = \frac{1}{2} \left(1 + \frac{2kd}{\sinh(2kd)} \right) \frac{\sigma}{k} + \bar{U}$$

$$c_\sigma = \frac{d\sigma}{dt} = \frac{\partial \sigma}{\partial d} \left[\frac{\partial d}{\partial t} + \bar{U} \cdot \nabla_{\bar{x}} d \right] - c_g \bar{k} \cdot \frac{\partial \bar{U}}{\partial s}$$

$$c_\theta = \frac{d\theta}{dt} = -\frac{1}{k} \left[\frac{\partial \sigma}{\partial d} \frac{\partial d}{\partial m} + \bar{k} \cdot \frac{\partial \bar{U}}{\partial m} \right]$$

Here, s is the space co-ordinate in wave direction θ and m is a co-ordinate perpendicular to s . $\nabla_{\bar{x}}$ is the two-dimensional differential operator in the \bar{x} -space.

Source Functions

The source function term, S , on the right hand side of the wave action conservation equation is given by

$$S = S_{in} + S_{nl} + S_{ds} + S_{bot} + S_{surf}$$

Here S_{in} represents the momentum transfer of wind energy to wave generation, S_{nl} the energy transfer due non-linear wave-wave interaction, S_{ds} the dissipation of wave energy due to white-capping (deep water wave breaking), S_{bot} the dissipation due to bottom friction and S_{surf} the dissipation of wave energy due to depth-induced breaking.

The default source functions S_{in} , S_{nl} and S_{ds} in MIKE 21 SW are similar to the source functions implemented in the WAM Cycle 4 model, see Komen et al (1994).

The wind input is based on Janssen's (1989, 1991) quasi-linear theory of wind-wave generation, where the momentum transfer from the wind to the sea not only depends on the wind stress, but also the sea state itself. The non-linear energy transfer (through the resonant four-wave interaction) is approximated by the DIA approach, Hasselmann et al (1985). The source function describing the dissipation due to white-capping is based on the theory of Hasselmann (1974) and Janssen (1989). The bottom friction dissipation is modelled using the approach by Johnson and Kofoed-Hansen (2000), which depends on the wave and sediment properties. The source function describing the bottom-induced wave breaking is based on the well-proven approach of Battjes and Janssen (1978) and Eldeberky and Battjes (1996).

A detailed description of the various source functions is available in Komen et al (1994) and Sørensen et al (2003), which also includes the references listed above.

Directional Decoupled Parametric Formulation

The directionally decoupled parametric formulation is based on a parameterisation of the wave action conservation equation. Following Holthuijsen et al (1989), the parameterisation is made in the frequency domain by introducing the zeroth and first moment of the wave action spectrum as dependent variables.

A similar formulation is used in the MIKE 21 NSW Near-shore Spectral Wind-Wave Model, which is one of the most popular models for wave transformation in coastal and shallow water environment. However, with MIKE 21 SW it is not necessary to set up a number of different orientated bathymetries to cover varying wind and wave directions.

The parameterisation leads to the following coupled equations

$$\frac{\partial(m_0)}{\partial t} + \frac{\partial(c_x m_0)}{\partial x} + \frac{\partial(c_y m_0)}{\partial y} + \frac{\partial(c_\theta m_0)}{\partial \theta} = T_0$$

$$\frac{\partial(m_1)}{\partial t} + \frac{\partial(c_x m_1)}{\partial x} + \frac{\partial(c_y m_1)}{\partial y} + \frac{\partial(c_\theta m_1)}{\partial \theta} = T_1$$

where $m_0(x, y, \theta)$ and $m_1(x, y, \theta)$ are the zeroth and first moment of the action spectrum $N(x, y, \sigma, \theta)$, respectively. $T_0(x, y, \theta)$ and $T_1(x, y, \theta)$ are source functions based on the action spectrum. The moments $m_n(x, y, \theta)$ are defined as

$$m_n(x, y, \theta) = \int_0^\infty \omega^n N(x, y, \omega, \theta) d\omega$$

The source functions T_0 and T_1 take into account the effect of local wind generation (stationary solution mode only) and energy dissipation due to bottom friction and wave breaking. The effects of wave-current interaction are also included. The source functions for the local wind generation are derived from empirical growth relations, see Johnson (1998) for details.

Numerical Methods

The frequency spectrum (fully spectral model only) is split into a prognostic part for frequencies lower than a cut-off frequency σ_{max} and an analytical diagnostic tail for the high-frequency part of the spectrum

$$E(\sigma, \theta) = E(\sigma_{max}, \theta) \left(\frac{\sigma}{\sigma_{max}} \right)^{-m}$$

where m is a constant ($= 5$) as proposed by Komen et al (1994).



The directional decoupled parametric formulation in MIKE 21 SW is used extensively for calculation of the wave transformation from deep-water to the shoreline and for wind-wave generation in local areas

Space Discretisation

The discretisation in geographical and spectral space is performed using cell-centred finite volume method. In the geographical domain an unstructured mesh is used. The spatial domain is discretised by subdivision of the continuum into non-overlapping elements. Triangle and quadrilateral shaped polygons are presently supported in MIKE 21 SW. The action density, $N(\sigma, \theta)$ is represented as a piecewise constant over the elements and stored at the geometric centres.

In frequency space either an equidistant or a logarithmic discretisation is used. In the directional space, an equidistant discretisation is used for both types of models. The action density is represented as piecewise constant over the discrete intervals, $\Delta\sigma$ and $\Delta\theta$, in the frequency and directional space.

Integrating the wave action conservation over an area A_i , the frequency interval $\Delta\sigma$ and the directional interval $\Delta\theta_m$ gives

$$\begin{aligned} & \frac{\partial}{\partial t} \int_{\Delta\theta_m} \int_{\Delta\sigma_l} \int_{A_i} N d\Omega d\sigma d\theta - \int_{\Delta\theta_m} \int_{\Delta\sigma_l} \int_{A_i} \frac{S}{\sigma} d\Omega d\sigma d\theta \\ & = \int_{\Delta\theta_m} \int_{\Delta\sigma_l} \int_{A_i} \nabla \cdot (\bar{v}N) d\Omega d\sigma d\theta \end{aligned}$$

where Ω is the integration variable defined on A_i . Using the divergence theorem and introducing the convective flux $\bar{F} = \bar{v}N$, we obtain

$$\begin{aligned} \frac{\partial N_{i,l,m}}{\partial t} & = -\frac{1}{A_i} \left[\sum_{p=1}^{NE} (F_n)_{p,l,m} \Delta l_p \right] \\ & - \frac{1}{\Delta\sigma_l} \left[(F_\sigma)_{i,l+1/2,m} - (F_\sigma)_{i,l-1/2,m} \right] \\ & - \frac{1}{\Delta\theta_m} \left[(F_\theta)_{i,l,m+1/2} - (F_\theta)_{i,l,m-1/2} \right] + \frac{S_{i,l,m}}{\sigma_l} \end{aligned}$$

where NE is the total number of edges in the cell, $(F_n)_{p,l,m} = (F_x n_x + F_y n_y)_{p,l,m}$ is the normal flux through the edge p in geographical space with length Δl_p . $(F_\sigma)_{i,l+1/2,m}$ and $(F_\theta)_{i,l,m+1/2}$ is the flux through the face in the frequency and directional space, respectively.

The convective flux is derived using a first-order upwinding scheme. In that

$$F_n = c_n \left(\frac{1}{2} (N_i + N_j) - \frac{1}{2} \frac{c}{|c|} (N_i - N_j) \right)$$

where c_n is the propagation speed normal to the element cell face.

Time Integration

The integration in time is based on a fractional step approach. Firstly, a propagation step is performed calculating an approximate solution N^* at the new time level $(n+1)$ by solving the homogenous wave action conservation equation, i.e. without the source terms. Secondly, a source terms step is performed calculating the new solution N^{n+1} from the estimated solution taking into account only the effect of the source terms.

The propagation step is carried out by an explicit Euler scheme

$$N_{i,l,m}^* = N_{i,l,m}^n + \Delta t \left(\frac{\partial N_{i,l,m}}{\partial t} \right)^n$$

To overcome the severe stability restriction, a multi-sequence integration scheme is employed. The maximum allowed time step is increased by employing a sequence of integration steps locally, where the number of steps may vary from point to point.

A source term step is performed using an implicit method (see Komen et al, 1994)

$$N_{i,l,m}^{n+1} = N_{i,l,m}^* + \Delta t \left[\frac{(1-\alpha)S_{i,l,m}^* + \alpha S_{i,l,m}^{n+1}}{\sigma_l} \right]$$

where α is a weighting coefficient that determines the type of finite difference method. Using a Taylor series to approximate S^{n+1} and assuming the off-diagonal terms in $\partial S / \partial E = \gamma$ are negligible, this equation can be simplified as

$$N_{i,l,m}^{n+1} = N_{i,l,m}^n + \frac{(S_{i,l,m}^* / \sigma_l) \Delta t}{(1 - \alpha \gamma \Delta t)}$$

For growing waves ($\gamma > 0$) an explicit forward difference is used ($\alpha = 0$), while for decaying waves ($\gamma < 0$) an implicit backward difference ($\alpha = 1$) is applied.



MIKE 21 SW is also applied for wave forecasts in ship route planning and improved service for conventional and fast ferry operators

Model Input

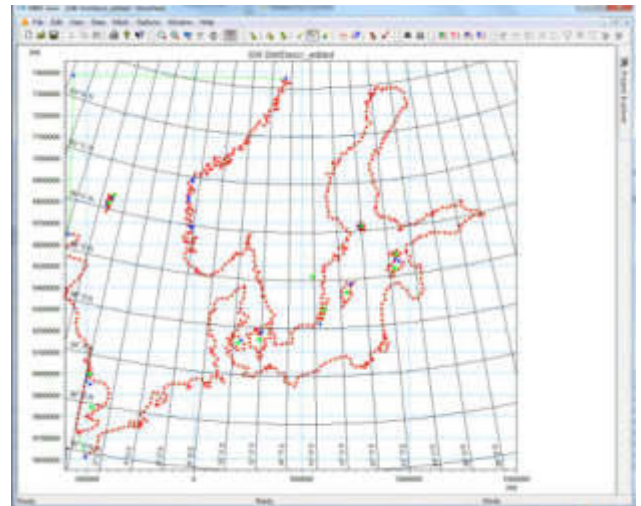
The necessary input data can be divided into following groups:

- Domain and time parameters:
 - computational mesh
 - co-ordinate type (Cartesian or spherical)
 - simulation length and overall time step
- Equations, discretisation and solution technique
 - formulation type
 - frequency and directional discretisation
 - number of time step groups
 - number of source time steps
- Forcing parameters
 - water level data
 - current data
 - wind data
 - ice data
- Source function parameters
 - non-linear energy transfer
 - wave breaking (shallow water)
 - bottom friction
 - white capping
- Structures
 - location and geometry
 - approach
 - structures coefficients
- Initial conditions
 - zero-spectrum (cold-start)
 - empirical data
 - data file
- Boundary conditions
 - closed boundaries
 - open boundaries (data format and type)

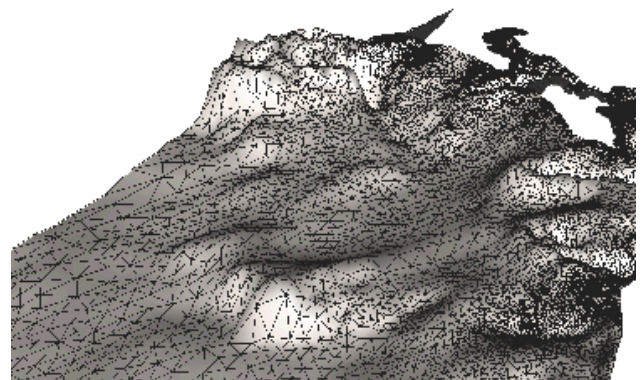
Providing MIKE 21 SW with a suitable mesh is essential for obtaining reliable results from the model. Setting up the mesh includes the appropriate selection of the area to be modelled, adequate resolution of the bathymetry, flow, wind and wave fields under consideration and definition of codes for essential and land boundaries.

Furthermore, the resolution in the geographical space must also be selected with respect to stability considerations.

As the wind is the main driving force in MIKE 21 SW, accurate hindcast or forecast wind fields are of utmost importance for the wave prediction.

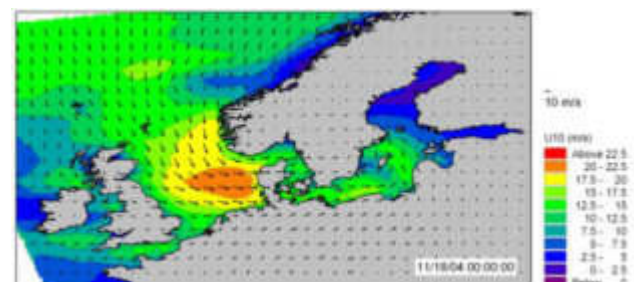


The Mesh Generator is an efficient MIKE Zero tool for the generation and handling of unstructured meshes, including the definition and editing of boundaries



3D visualisation of a computational mesh

If wind data is not available from an atmospheric meteorological model, the wind fields (e.g. cyclones) can be determined by using the wind-generating programs available in MIKE 21 Toolbox.

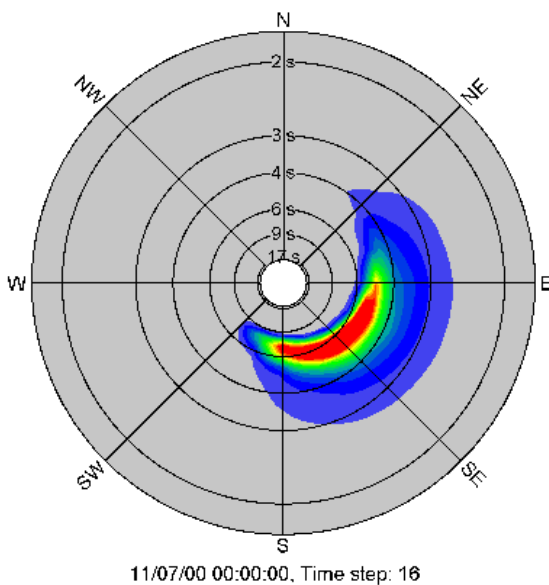


The chart shows an example of a wind field covering the North Sea and Baltic Sea as wind speed and wind direction. This is used as input to MIKE 21 SW in forecast and hindcast mode

Model Output

At each mesh point and for each time step four types of output can be obtained from MIKE 21 SW:

- Integral wave parameters divided into wind sea and swell such as
 - significant wave height, H_{m0}
 - peak wave period, T_p
 - averaged wave period, T_{01}
 - zero-crossing wave period, T_{02}
 - wave energy period, T_{-10}
 - peak wave direction, θ_p
 - mean wave direction, θ_m
 - directional standard deviation, σ
 - wave height with dir., $H_{m0} \cos\theta_m$, $H_{m0} \sin\theta_m$
 - radiation stress tensor, S_{xx} , S_{xy} and S_{yy}
 - particle velocities, *horizontal/vertical*
 - wave power, P , P_x and P_y



Example of model output (directional-frequency wave spectrum) processed using the Polar Plot control in the MIKE Zero Plot Composer

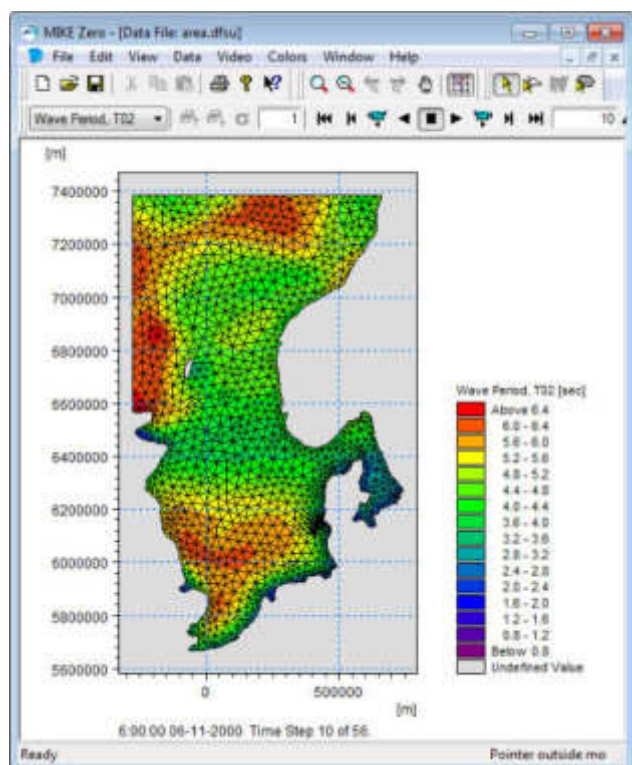
The distinction between wind-sea and swell can be calculated using either a constant threshold frequency or a dynamic threshold frequency with an upper frequency limit.

- Input parameters
 - water level, WL
 - water depth, h
 - current velocity, \bar{U}
 - wind speed, U_{10}
 - wind direction, θ_w
 - Ice concentration

- Model parameters
 - bottom friction coefficient, C_f
 - breaking parameter, γ
 - Courant number, Cr
 - time step factor, α
 - characteristic edge length, Δl
 - area of element, a
 - wind friction speed, u^*
 - roughness length, z_0
 - drag coefficient, C_D
 - Charnock parameter, z_{ch}
- Directional-frequency wave spectra at selected grid points and or areas as well as direction spectra and frequency spectra

Output from MIKE 21 SW is typically post-processed using the Data Viewer available in the common MIKE Zero shell. The Data Viewer is a tool for analysis and visualisation of unstructured data, e.g. to view meshes, spectra, bathymetries, results files of different format with graphical extraction of time series and line series from plan view and import of graphical overlays.

Various other editors and plot controls in the MIKE Zero Composer (e.g. Time Series Plot, Polar Plot, etc.) can be used for analysis and visualisation.



The Data Viewer in MIKE Zero – an efficient tool for analysis and visualisation of unstructured data including processing of animations

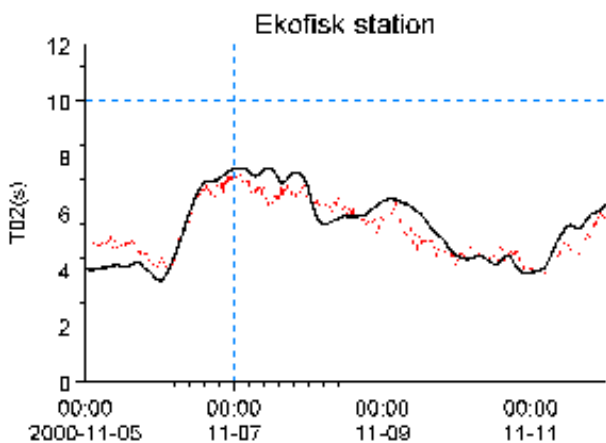
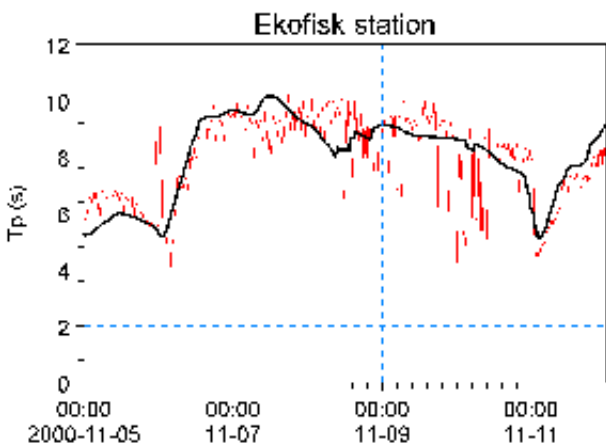
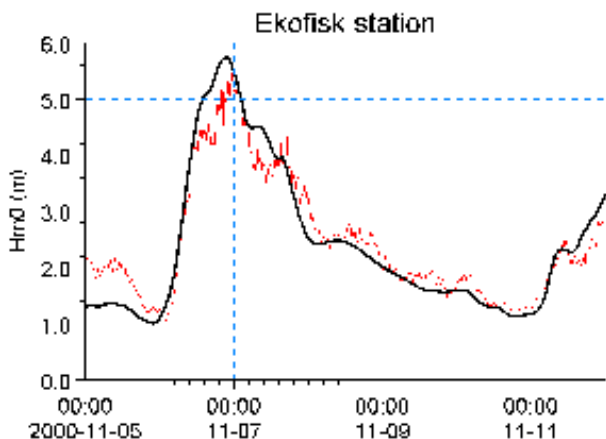
Validation

The model has successfully been applied to a number of rather basic idealised situations for which the results can be compared with analytical solutions or information from the literature. The basic tests covered fundamental processes such as wave propagation, depth-induced and current-induced shoaling and refraction, wind-wave generation and dissipation.

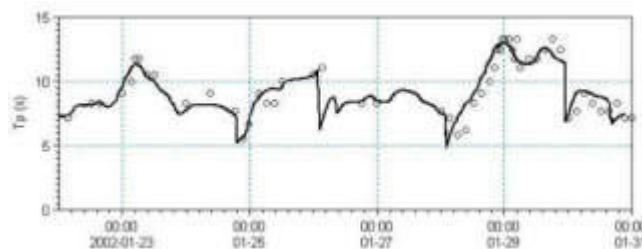
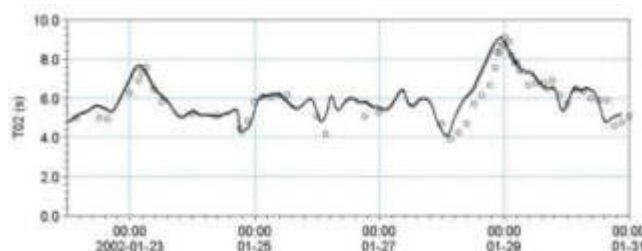
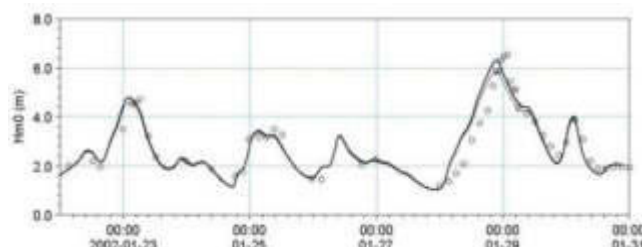


A major application area of MIKE 21 SW is in connection with design and maintenance of offshore structures

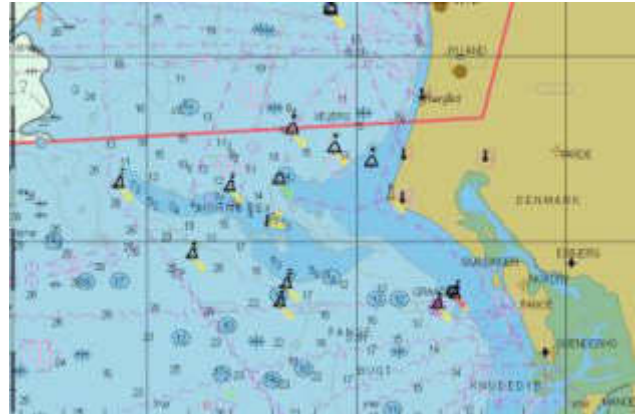
The model has also been tested in natural geophysical conditions (e.g. in the North Sea, the Danish West Coast and the Baltic Sea), which are more realistic and complicated than the academic test and laboratory tests mentioned above.



Comparison between measured and simulated significant wave height, peak wave period and mean wave period at the Ekofisk offshore platform (water depth 70 m) in the North Sea). (—) calculations and (---) measurements

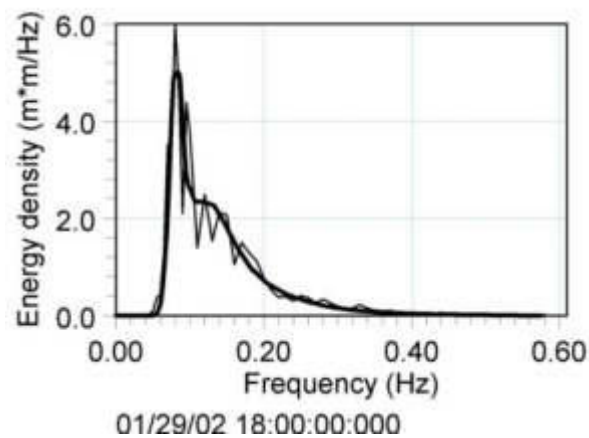
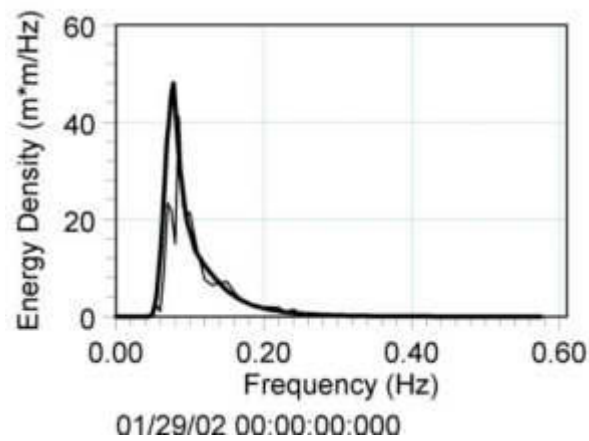


Comparison between measured and simulated significant wave height, peak wave period and mean wave period at Fjaltring located at the Danish west coast (water depth 17.5 m). (—) calculations and (o) measurements

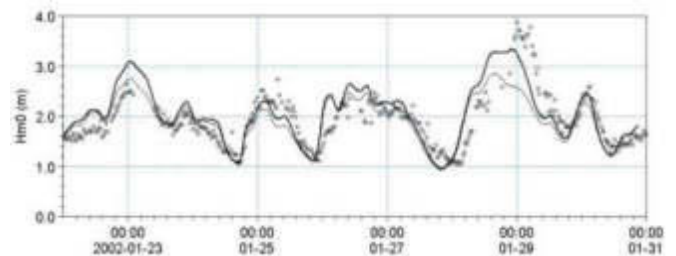
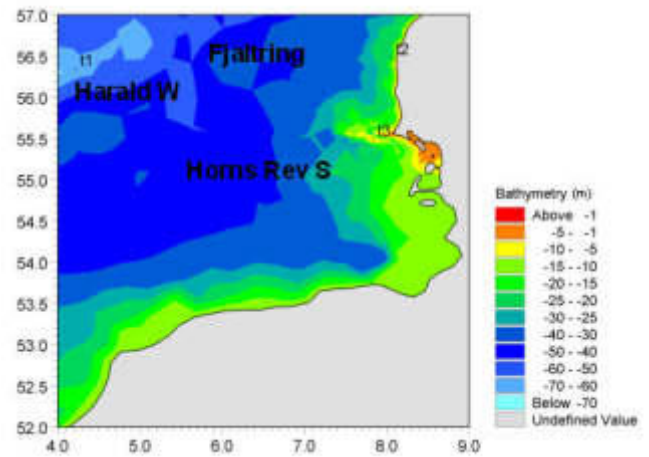


The Fjaltring directional wave rider buoy is located offshore relative to the depicted arrow

MIKE 21 SW is used for prediction of the wave conditions at the complex Horns Rev (reef) in the southeastern part of the North Sea. At this site, a 168 MW offshore wind farm with 80 turbines has been established in water depths between 6.5 and 13.5 m.

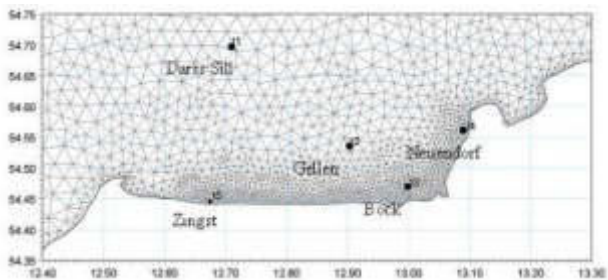
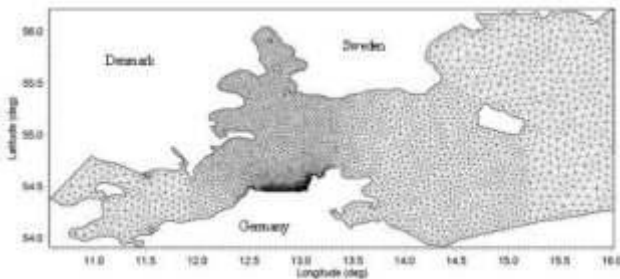
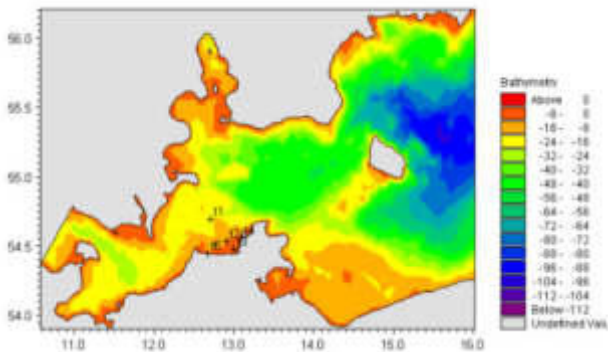


Comparison of frequency spectra at Fjaltring. (—) calculations and (—) measurements

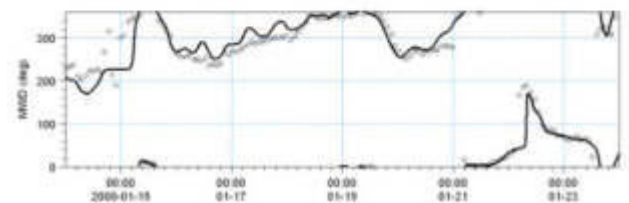
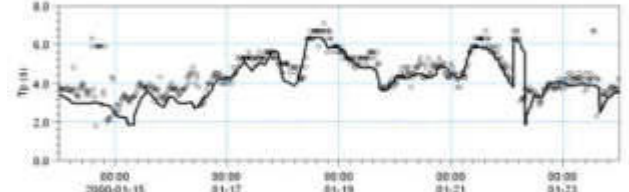
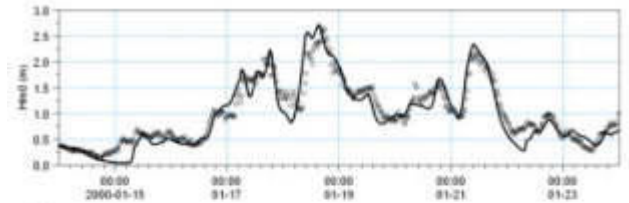


The upper panels show the Horns Rev offshore wind farm and MIKE C-map chart. The middle panel shows a close-up of the mesh near the Horns Rev S wave rider buoy (t3, 10 m water depth). The lower panel shows a comparison between measured and simulated significant wave height at Horns Rev S, (—) calculations including tide and surge and (---) calculations excluding including tide and surge, (o) measurements

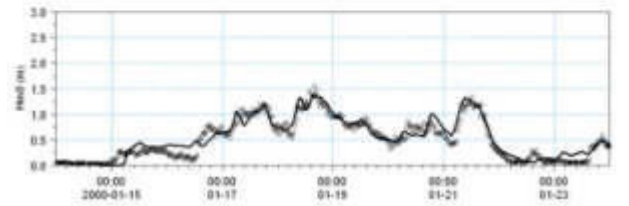
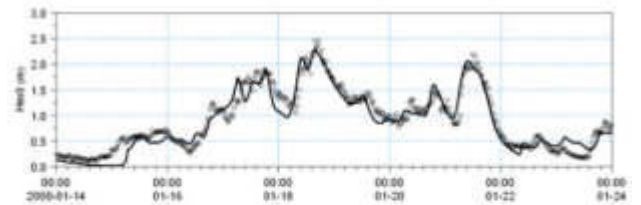
The predicted nearshore wave climate along the island of Hiddensee and the coastline of Zingst located in the micro-tidal Gellen Bay, Germany have been compared to field measurements (Sørensen et al, 2004) provided by the MORWIN project. From the illustrations it can be seen that the wave conditions are well reproduced both offshore and in more shallow water near the shore. The RMS values (on significant wave height) are less than 0.25m at all five stations.



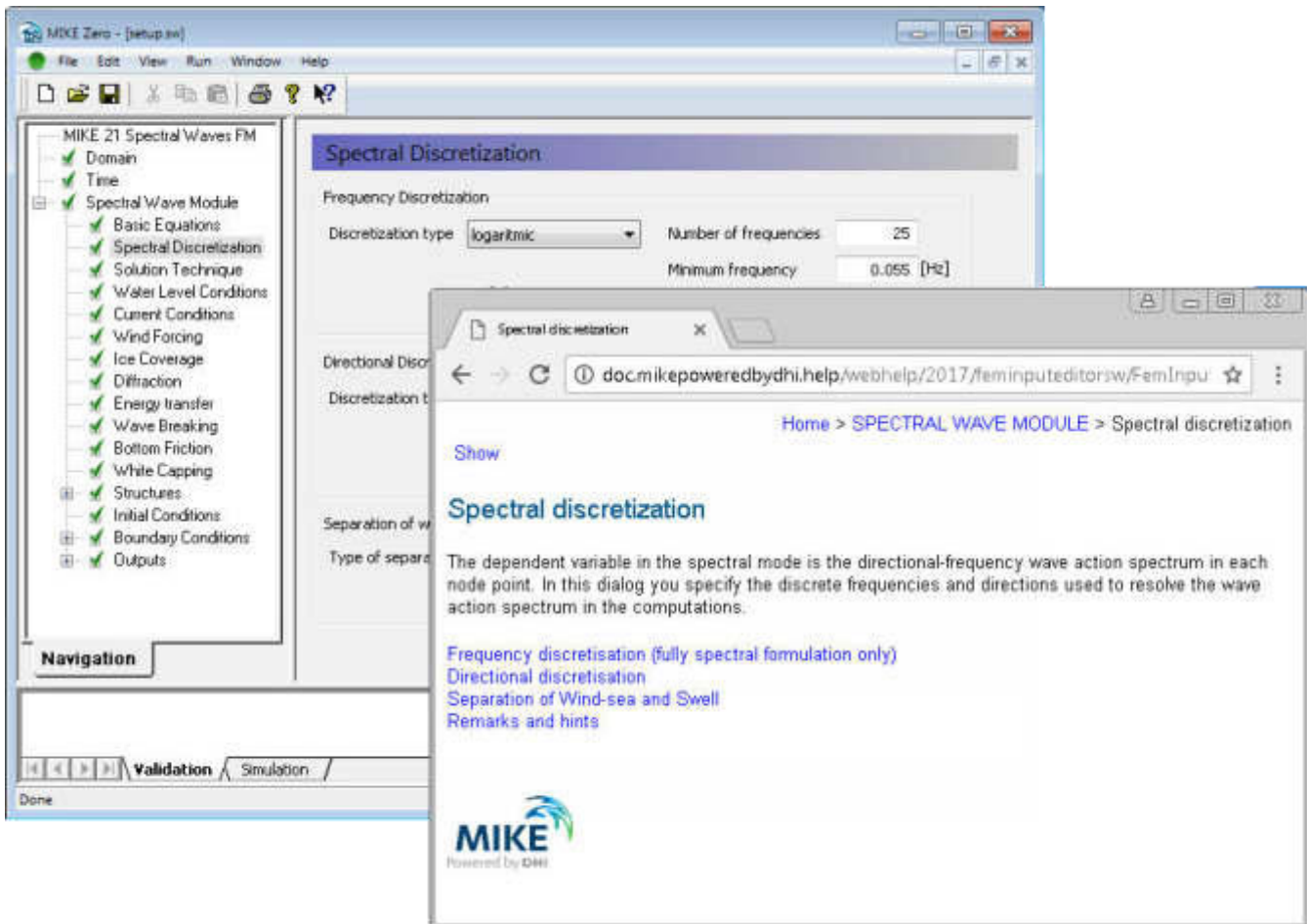
A MIKE 21 SW hindcast application in the Baltic Sea. The upper chart shows the bathymetry and the middle and lower charts show the computational mesh. The lower chart indicates the location of the measurement stations



Time series of significant wave height, H_{m0} , peak wave period, T_p , and mean wave direction, MWD, at Darss sill (Offshore, depth 20.5 m). (—) Calculation and (o) measurements. The RMS value on H_{m0} is approximately 0.2 m



Time series of significant wave height, H_{m0} , at Gellen (upper, depth 8.3m) and Bock (lower, depth 5.5 m). (—) Calculation and (o) measurements. The RMS value on H_{m0} is approximately 0.15 m

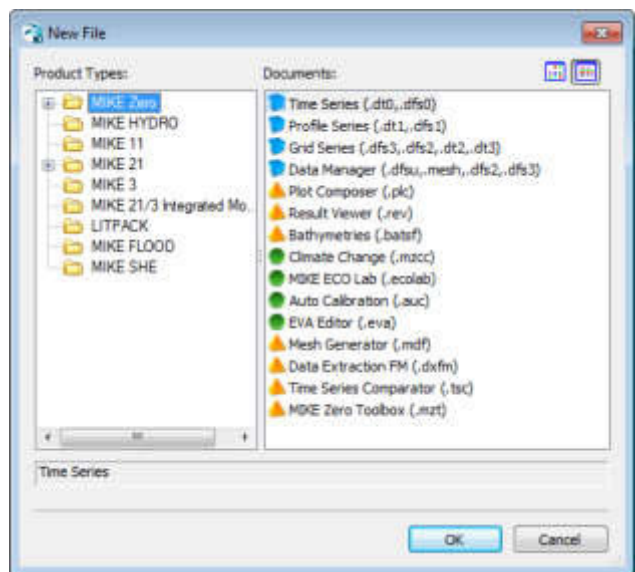


Graphical user interface of MIKE 21 SW, including an example of the Online Help System

Graphical User Interface

MIKE 21 SW is operated through a fully Windows integrated Graphical User Interface (GUI). Support is provided at each stage by an Online Help System.

The common MIKE Zero shell provides entries for common data file editors, plotting facilities and a toolbox for/utilities as the Mesh Generator and Data Viewer.



Overview of the common MIKE Zero utilities

FEMA Approval of MIKE 21

The US Federal Emergency Management Agency (FEMA) has per May 2001 officially approved MIKE 21 for use in coastal Flood Insurance Studies.

The three modules, which are the hydro-dynamic module, near-shore spectral wind-wave module and offshore-spectral wind-wave module, have been accepted for coastal storm surge, coastal wave heights, and coastal wave effect usage.

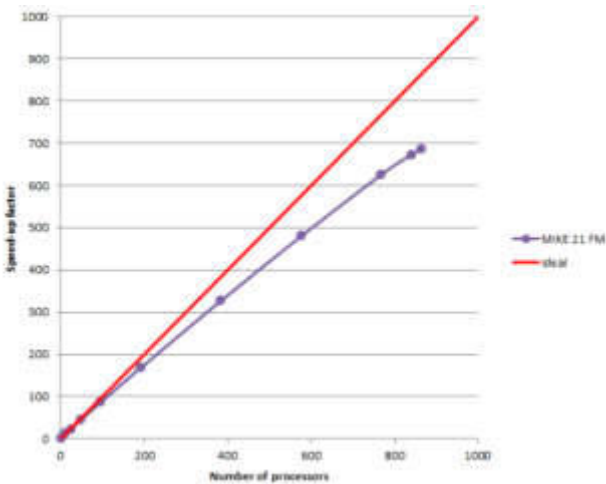
For more information please check www.fema.gov/ifp and www.dhisoftware.com.



FEMA approval of the MIKE 21 package

Parallelisation

The computational engines of the MIKE 21/3 FM series are available in versions that have been parallelised using both shared memory as well as distributed memory architecture. The latter approach allows for domain decomposition. The result is much faster simulations on systems with many cores.



Example of MIKE 21 HD FM speed-up using a HPC Cluster with distributed memory architecture (purple)

Hardware and Operating System Requirements

The MIKE Zero Modules support Microsoft Windows 7 Professional Service Pack 1 (64 bit), Windows 10 Pro (64 bit), Windows Server 2012 R2 Standard (64 bit) and Windows Server 2016 Standard (64 bit).

Microsoft Internet Explorer 9.0 (or higher) is required for network license management. An internet browser is also required for accessing the web-based documentation and online help.

The recommended minimum hardware requirements for executing the MIKE Zero modules are:

Processor:	3 GHz PC (or higher)
Memory (RAM):	2 GB (or higher)
Hard disk:	40 GB (or higher)
Monitor:	SVGA, resolution 1024x768
Graphics card:	64 MB RAM (256 MB RAM or higher is recommended)

Support

News about new features, applications, papers, updates, patches, etc. are available here:

www.mikepoweredbydhi.com/Download/DocumentsAndTools.aspx

For further information on MIKE 21 SW, please contact your local DHI office or the support centre:

MIKE Powered by DHI Client Care
 Agern Allé 5
 DK-2970 Hørsholm
 Denmark

Tel: +45 4516 9333

Fax: +45 4516 9292

mike@dhigroup.com

www.mikepoweredbydhi.com

Documentation

The MIKE 21 & MIKE 3 FM models are provided with comprehensive user guides, online help, scientific documentation, application examples and step-by-step training examples.

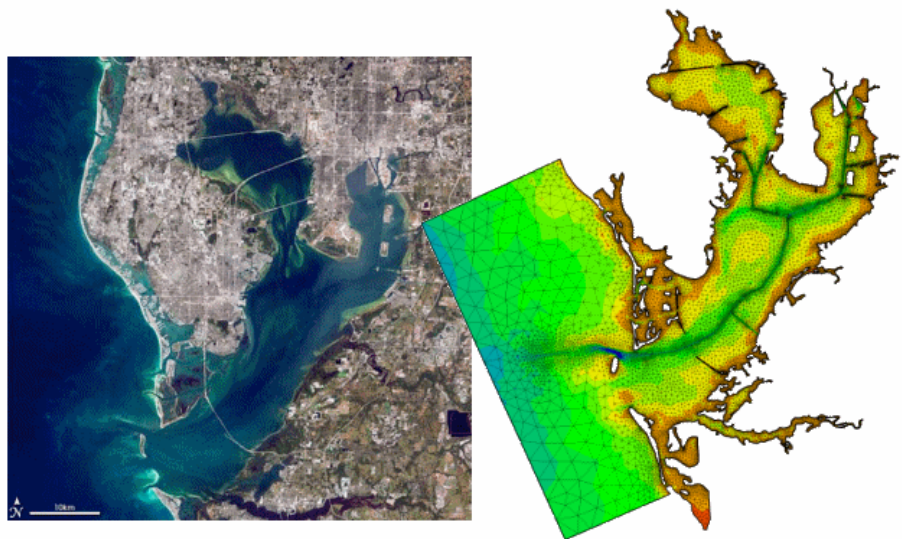


References

- Sørensen, O. R., Kofoed-Hansen, H., Rugbjerg, M. and Sørensen, L.S., (2004): A Third Generation Spectral Wave Model Using an Unstructured Finite Volume Technique. In Proceedings of the 29th International Conference of Coastal Engineering, 19-24 September 2004, Lisbon, Portugal.
- Johnson, H.K., and Kofoed-Hansen, H., (2000). Influence of bottom friction on sea surface roughness and its impact on shallow water wind wave modelling. *J. Phys. Oceanog.*, **30**, 1743-1756.
- Johnson, H.K., Vested, H.J., Hersbach, H. Højstrup, J. and Larsen, S.E., (1999). On the coupling between wind and waves in the WAM model. *J. Atmos. Oceanic Technol.*, **16**, 1780-1790.
- Johnson, H.K. (1998). On modeling wind-waves in shallow and fetch limited areas using the method of Holthuijsen, Booij and Herbers. *J. Coastal Research*, **14**, 3, 917-932.
- Young, I.R., (1999). Wind generated ocean waves, in Elsevier Ocean Engineering Book Series, Volume 2, Eds. R. Bhattacharyya and M.E. McCormick, Elsevier.
- Komen, G.J., Cavaleri, L., Doneland, M., Hasselmann, K., Hasselmann S. and Janssen, P.A.E.M., (1994). Dynamics and modelling of ocean waves. Cambridge University Press, UK, 560 pp.
- Holthuijsen, L.H, Booij, N. and Herbers, T.H.C. (1989). A prediction model for stationary, short-crested waves in shallow water with ambient currents, *Coastal Engr.*, **13**, 23-54.

References on Applications

- Kofoed-Hansen, H., Johnson, H.K., Højstrup, J. and Lange, B., (1998). Wind-wave modelling in waters with restricted fetches. In: Proc of 5th International Workshop on Wave Hindcasting and Forecasting, 27-30 January 1998, Melbourne, FL, USA, pp. 113-127.
- Kofoed-Hansen, H, Johnson, H.K., Astrup, P. and Larsen, J., (2001). Prediction of waves and sea surface roughness in restricted coastal waters. In: Proc of 27th International Conference of Coastal Engineering, pp.1169-1182.
- Al-Mashouk, M.A., Kerper, D.R. and Jacobsen, V., (1998). Red Sea Hindcast study: Development of a sea state design database for the Red Sea.. *J Saudi Aramco Technology*, **1**, 10 pp.
- Rugbjerg, M., Nielsen, K., Christensen, J.H. and Jacobsen, V., (2001). Wave energy in the Danish part of the North Sea. In: Proc of 4th European Wave Energy Conference, 8 pp.



MIKE 21 & MIKE 3 Flow Model FM

Hydrodynamic Module

Short Description



DHI headquarters

Agern Allé 5
DK-2970 Hørsholm
Denmark

+45 4516 9200 Telephone
+45 4516 9333 Support
+45 4516 9292 Telefax

mike@dhigroup.com
www.mikepoweredbydhi.com

MIKE 21 & MIKE 3 Flow Model FM

The Flow Model FM is a comprehensive modelling system for two- and three-dimensional water modelling developed by DHI. The 2D and 3D models carry the same names as the classic DHI model versions MIKE 21 & MIKE 3 with an 'FM' added referring to the type of model grid - Flexible Mesh.

The modelling system has been developed for complex applications within oceanographic, coastal and estuarine environments. However, being a general modelling system for 2D and 3D free-surface flows it may also be applied for studies of inland surface waters, e.g. overland flooding and lakes or reservoirs.



MIKE 21 & MIKE 3 Flow Model FM is a general hydrodynamic flow modelling system based on a finite volume method on an unstructured mesh

The Modules of the Flexible Mesh Series

DHI's Flexible Mesh (FM) series includes the following modules:

Flow Model FM modules

- Hydrodynamic Module, HD
- Transport Module, TR
- Ecology Modules, MIKE ECO Lab/AMB Lab
- Oil Spill Module, OS
- Mud Transport Module, MT
- Particle Tracking Module, PT
- Sand Transport Module, ST
- Shoreline Morphology Module, SM

Wave module

- Spectral Wave Module, SW

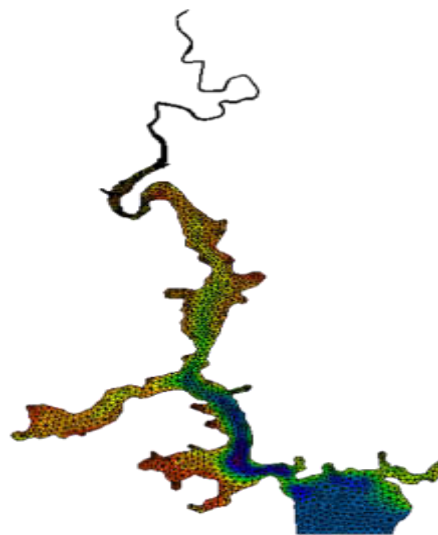
The FM Series meets the increasing demand for realistic representations of nature, both with regard to 'look alike' and to its capability to model coupled processes, e.g. coupling between currents, waves and sediments. Coupling of modules is managed in the Coupled Model FM.

All modules are supported by advanced user interfaces including efficient and sophisticated tools for mesh generation, data management, 2D/3D visualization, etc. In combination with comprehensive documentation and support, the FM series forms a unique professional software tool for consultancy services related to design, operation and maintenance tasks within the marine environment.

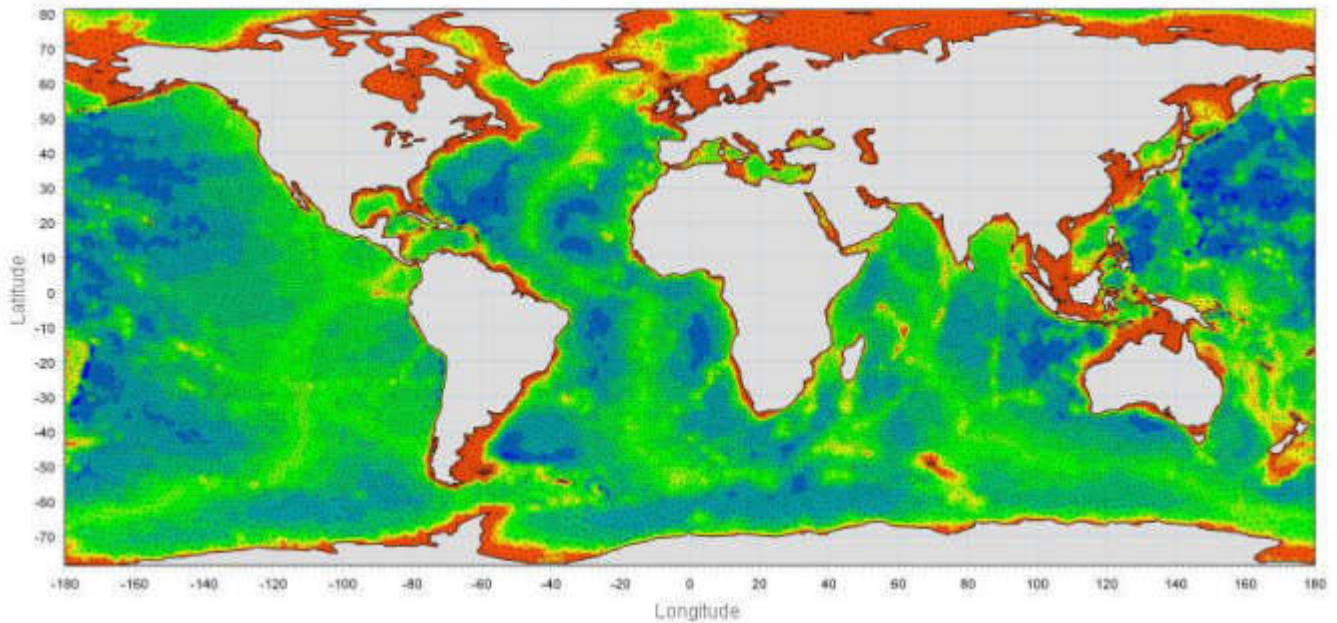
An unstructured grid provides an optimal degree of flexibility in the representation of complex geometries and enables smooth representations of boundaries. Small elements may be used in areas where more detail is desired, and larger elements used where less detail is needed, optimising information for a given amount of computational time.

The spatial discretisation of the governing equations is performed using a cell-centred finite volume method. In the horizontal plane, an unstructured grid is used while a structured mesh is used in the vertical domain (3D).

This document provides a short description of the Hydrodynamic Module included in MIKE 21 & MIKE 3 Flow Model FM.



Example of computational mesh for Tamar Estuary, UK



MIKE 21 & MIKE 3 FLOW MODEL FM supports both Cartesian and spherical coordinates. Spherical coordinates are usually applied for regional and global sea circulation applications. The chart shows the computational mesh and bathymetry for the planet Earth generated by the MIKE Zero Mesh Generator

MIKE 21 & MIKE 3 Flow Model FM - Hydrodynamic Module

The Hydrodynamic Module provides the basis for computations performed in many other modules, but can also be used alone. It simulates the water level variations and flows in response to a variety of forcing functions on flood plains, in lakes, estuaries and coastal areas.

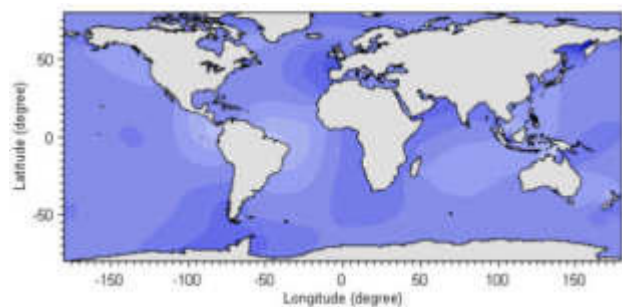
Application Areas

The Hydrodynamic Module included in MIKE 21 & MIKE 3 Flow Model FM simulates unsteady flow taking into account density variations, bathymetry and external forcings.

The choice between 2D and 3D model depends on a number of factors. For example, in shallow waters, wind and tidal current are often sufficient to keep the water column well-mixed, i.e. homogeneous in salinity and temperature. In such cases a 2D model can be used. In water bodies with stratification, either by density or by species (ecology), a 3D model should be used. This is also the case for enclosed or semi-enclosed waters where wind-driven circulation occurs.

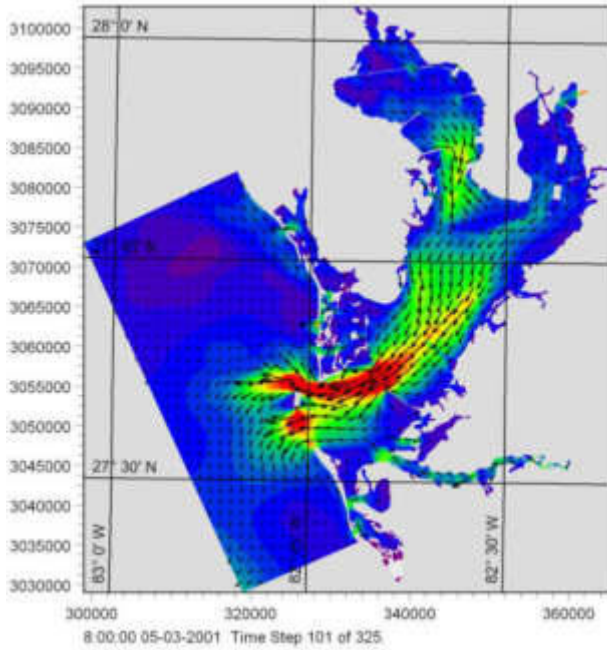
Typical application areas are

- Assessment of hydrographic conditions for design, construction and operation of structures and plants in stratified and non-stratified waters
- Environmental impact assessment studies
- Coastal and oceanographic circulation studies
- Optimization of port and coastal protection infrastructures
- Lake and reservoir hydrodynamics
- Cooling water, recirculation and desalination
- Coastal flooding and storm surge
- Inland flooding and overland flow modelling
- Forecast and warning systems



Example of a global tide application of MIKE 21 Flow Model FM. Results from such a model can be used as boundary conditions for regional scale forecast or hindcast models

The MIKE 21 & MIKE 3 Flow Model FM also support spherical coordinates, which makes both models particularly applicable for global and regional sea scale applications.

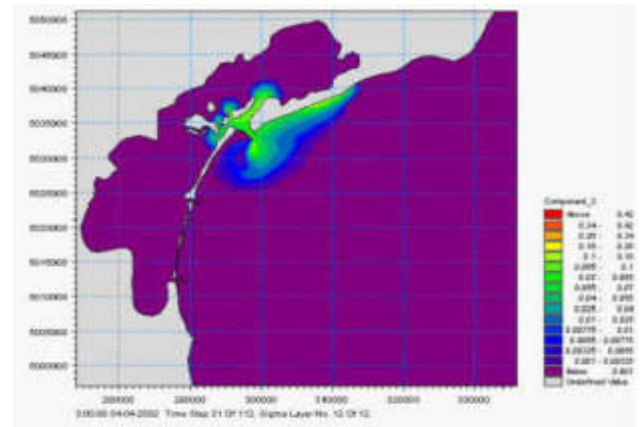


Example of a flow field in Tampa Bay, Florida, simulated by MIKE 21 Flow Model FM

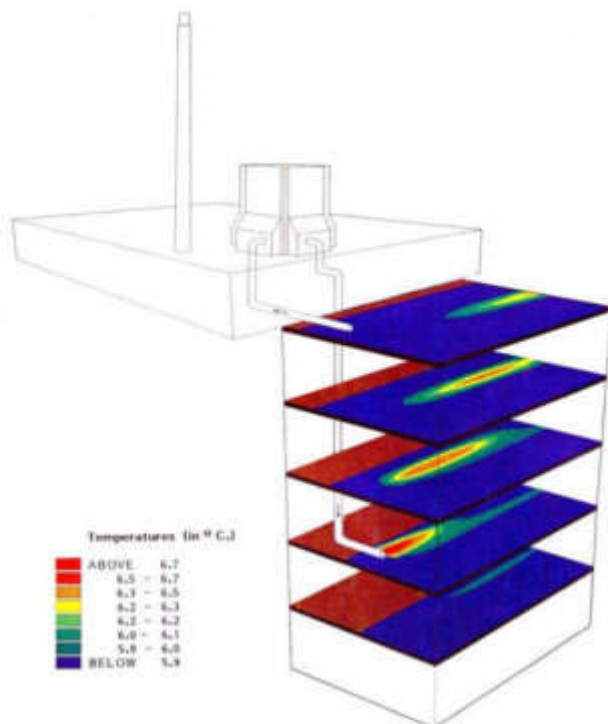


Typical applications with the MIKE 21 & MIKE 3 Flow Model FM include cooling water recirculation and ecological impact assessment (eutrophication)

The Hydrodynamic Module is together with the Transport Module (TR) used to simulate the spreading and fate of dissolved and suspended substances. This module combination is applied in tracer simulations, flushing and simple water quality studies.



Tracer simulation of single component from outlet in the Adriatic, simulated by MIKE 21 Flow Model FM HD+TR



Study of thermal plume dispersion

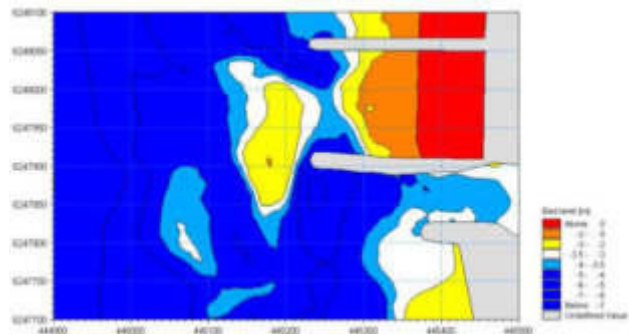


Prediction of ecosystem behaviour using the MIKE 21 & MIKE 3 Flow Model FM together with MIKE ECO Lab

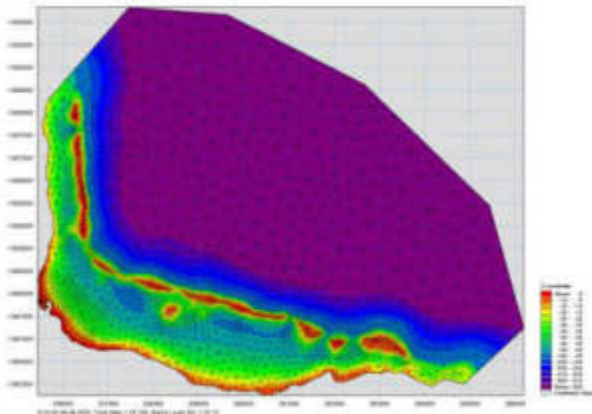
The Hydrodynamic Module can be coupled to the Ecological Module (MIKE ECO Lab) to form the basis for environmental water quality studies comprising multiple components.

Furthermore, the Hydrodynamic Module can be coupled to sediment models for the calculation of sediment transport. The Sand Transport Module and Mud Transport Module can be applied to simulate transport of non-cohesive and cohesive sediments, respectively.

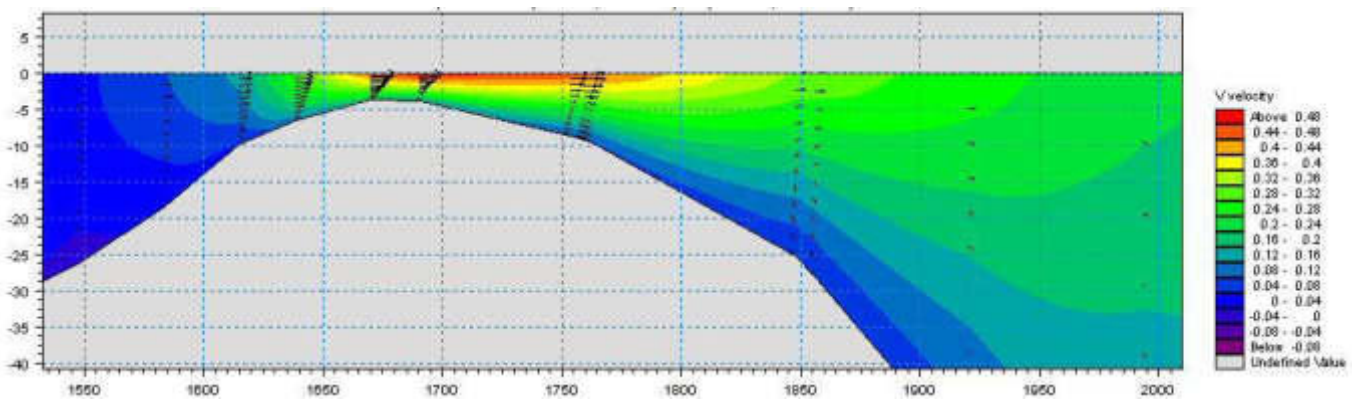
In the coastal zone the transport is mainly determined by wave conditions and associated wave-induced currents. The wave-induced currents are generated by the gradients in radiation stresses that occur in the surf zone. The Spectral Wave Module can be used to calculate the wave conditions and associated radiation stresses.



Coastal application (morphology) with coupled MIKE 21 HD, SW and ST, Torsminde harbour Denmark



Model bathymetry of Taravao Bay, Tahiti



Example of vertical profile of cross reef currents in Taravao Bay, Tahiti simulated with MIKE 3 Flow Model FM. The circulation and renewal of water inside the reef is dependent on the tides, the meteorological conditions and the cross reef currents, thus the circulation model includes the effects of wave induced cross reef currents

Computational Features

The main features and effects included in simulations with the MIKE 21 & MIKE 3 Flow Model FM – Hydrodynamic Module are the following:

- Flooding and drying
- Momentum dispersion
- Bottom shear stress
- Coriolis force
- Wind shear stress
- Barometric pressure gradients
- Ice coverage
- Tidal potential
- Precipitation/evaporation
- Infiltration
- Heat exchange with atmosphere
- Wave radiation stresses
- Sources and sinks, incl. jet
- Structures

Model Equations

The modelling system is based on the numerical solution of the two/three-dimensional incompressible Reynolds averaged Navier-Stokes equations subject to the assumptions of Boussinesq and of hydrostatic pressure. Thus, the model consists of continuity, momentum, temperature, salinity and density equations and it is closed by a turbulent closure scheme. The density does not depend on the pressure, but only on the temperature and the salinity.

For the 3D model, the free surface is taken into account using a sigma-coordinate transformation approach or using a combination of a sigma and z-level coordinate system.

Below the governing equations are presented using Cartesian coordinates.

The local continuity equation is written as

$$\frac{\partial u}{\partial x} + \frac{\partial v}{\partial y} + \frac{\partial w}{\partial z} = S$$

and the two horizontal momentum equations for the x- and y-component, respectively

$$\frac{\partial u}{\partial t} + \frac{\partial u^2}{\partial x} + \frac{\partial vu}{\partial y} + \frac{\partial wu}{\partial z} = fv - g \frac{\partial \eta}{\partial x} -$$

$$\frac{1}{\rho_0} \frac{\partial p_a}{\partial x} - \frac{g}{\rho_0} \int_z^\eta \frac{\partial \rho}{\partial x} dz + F_u + \frac{\partial}{\partial z} \left(\nu_t \frac{\partial u}{\partial z} \right) + u_s S$$

$$\frac{\partial v}{\partial t} + \frac{\partial v^2}{\partial y} + \frac{\partial uv}{\partial x} + \frac{\partial wv}{\partial z} = -fu - g \frac{\partial \eta}{\partial y} -$$

$$\frac{1}{\rho_0} \frac{\partial p_a}{\partial y} - \frac{g}{\rho_0} \int_z^\eta \frac{\partial \rho}{\partial y} dz + F_v + \frac{\partial}{\partial z} \left(\nu_t \frac{\partial v}{\partial z} \right) + v_s S$$

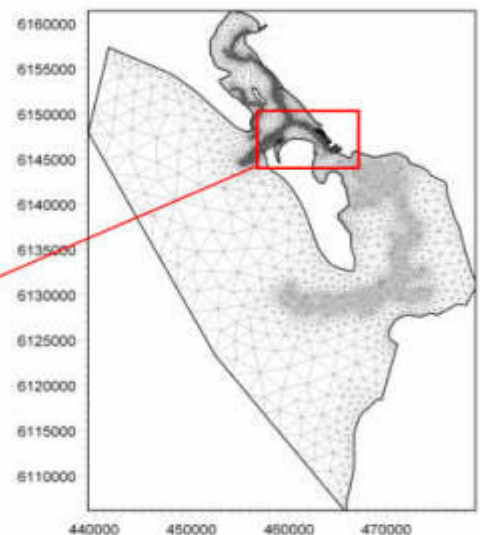
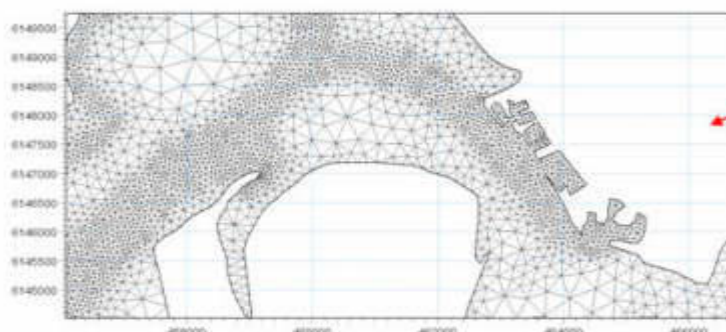
Temperature and salinity

In the Hydrodynamic Module, calculations of the transports of temperature, T , and salinity, s follow the general transport-diffusion equations as

$$\frac{\partial T}{\partial t} + \frac{\partial uT}{\partial x} + \frac{\partial vT}{\partial y} + \frac{\partial wT}{\partial z} = F_T + \frac{\partial}{\partial z} \left(D_v \frac{\partial T}{\partial z} \right) + \hat{H} + T_s S$$

$$\frac{\partial s}{\partial t} + \frac{\partial us}{\partial x} + \frac{\partial vs}{\partial y} + \frac{\partial ws}{\partial z} = F_s + \frac{\partial}{\partial z} \left(D_v \frac{\partial s}{\partial z} \right) + s_s S$$

Unstructured mesh technique gives the maximum degree of flexibility, for example: 1) Control of node distribution allows for optimal usage of nodes 2) Adoption of mesh resolution to the relevant physical scales 3) Depth-adaptive and boundary-fitted mesh. Below is shown an example from Ho Bay, Denmark with the approach channel to the Port of Esbjerg



The horizontal diffusion terms are defined by

$$(F_T, F_s) = \left[\frac{\partial}{\partial x} \left(D_h \frac{\partial}{\partial x} \right) + \frac{\partial}{\partial y} \left(D_h \frac{\partial}{\partial y} \right) \right] (T, s)$$

The equations for two-dimensional flow are obtained by integration of the equations over depth.

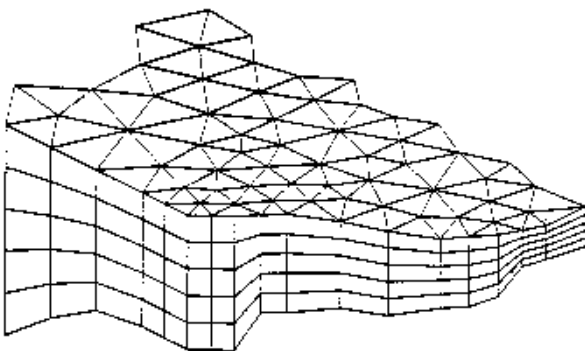
Heat exchange with the atmosphere is also included.

Symbol list

t	time
x, y, z	Cartesian coordinates
u, v, w	flow velocity components
T, s	temperature and salinity
D_v	vertical turbulent (eddy) diffusion coefficient
\hat{H}	source term due to heat exchange with atmosphere
S	magnitude of discharge due to point sources
T_s, s_s	temperature and salinity of source
F_T, F_s, F_c	horizontal diffusion terms
D_h	horizontal diffusion coefficient
h	depth

Solution Technique

The spatial discretisation of the primitive equations is performed using a cell-centred finite volume method. The spatial domain is discretised by subdivision of the continuum into non-overlapping elements/cells.



Principle of 3D mesh

In the horizontal plane an unstructured mesh is used while a structured mesh is used in the vertical domain of the 3D model. In the 2D model the elements can be triangles or quadrilateral elements. In the 3D model the elements can be prisms or bricks whose horizontal faces are triangles and quadrilateral elements, respectively.

The effect of a number of structure types (weirs, culverts, dikes, gates, piers and turbines) with a horizontal dimension which usually cannot be resolved by the computational mesh is modelled by a subgrid technique.

Model Input

Input data can be divided into the following groups:

- Domain and time parameters:
 - computational mesh (the coordinate type is defined in the computational mesh file) and bathymetry
 - simulation length and overall time step
- Calibration factors
 - bed resistance
 - momentum dispersion coefficients
 - wind friction factors
 - heat exchange coefficients
- Initial conditions
 - water surface level
 - velocity components
 - temperature and salinity
- Boundary conditions
 - closed
 - water level
 - discharge
 - temperature and salinity
- Other driving forces
 - wind speed and direction
 - tide
 - source/sink discharge
 - wave radiation stresses
- Structures
 - Structure type
 - location
 - structure data